SOUR GAS INJECTION TO ENHANCE OIL RECOVERY

A thesis presented to the Department of Petroleum Engineering

African University of Science and Technology

In partial fulfillment of the requirements for the degree of

MASTER OF SCIENCE IN PETROLEUM ENGINEERING

By

AMINU YAU KAITA

Supervised by

Dr. Xingru Wu

African University of Science and Technology
www.aust.edu.ng
P.M.B 681, Garki, Abuja F.C.T
Nigeria

February, 2018

CERTIFICATION

This is to certify that the thesis titled "**SOUR GAS INJECTION TO ENHANCE OIL RECOVERY**" submitted to the school of postgraduate studies, African University of Science and Technology (AUST), Abuja, Nigeria for the award of the Master's degree is a record of original research carried out by Aminu Yau Kaita in the Department of Petroleum Engineering.

SOUR GAS INJECTION TO ENHANCE OIL RECOVERY

By

Aminu Yau Kaita

A THESIS APPROVED BY THE PETROLEUM ENGINEERING DEPARTMENT

RECOMMENDED:

Supervisor, Dr. Xingru Wu

Co-supervisor,

Co-supervisor

Head, Department of Petroleum Engineering

APPROVED:

Chief Academic Officer

Date

ABSTRACT

Proper handling of sour gas produced is crucial to the development of sour reservoirs. Over years of research and practice, many methods of sour gas processing have been developed from the solid storage of sulfur to reinjecting the sour gas back into producing or depleted light oil reservoir for miscible flooding enhanced oil recovery. This paper seeks to investigate the use of sour gas to enhance oil recovery and its associated phase behavior problems.

In designing a miscible gas flooding project, the minimum miscibility pressure (MMP) is the key parameter that determines the impact on gas and oil mixing phase behavior. The MMP is the lowest pressure at which the displacement process becomes miscible upon contact with the reservoir fluid. There are various methods to determine the MMP. A laboratory experiment is the most accurate but time consuming and subject to fluid sample quality; while the Equation of State is poor in characterizing polar molecules like H_2S. For this study, empirical correlations are used to determine the MMP because the study focuses more on the general trend of how methane concentration affects the MMP of the process.

In this study, a sour gas injection model is developed using a compositional simulator with the aim to determine mechanistically how sour gas enhances oil recovery. This model is used to evaluate the effect of some important parameters such as acid gas concentration, injection pressure and injection rates on oil recovery efficiency.

The result of MMP study shows that methane concentration has a significant impact on the MMP of the process. As methane concentration increases in the injection gas, the MMP of the process also increases. From this study, it was observed that increasing acid gas concentration decreases the MMP of the process as a result of an increase in gas viscosity, consequently extending the plateau period resulting in late gas breakthrough and increasing the overall recovery of the process. It is also seen that this increase in viscosity increases the

volumetric sweep efficiency of the process which is an improvement to most gas injection enhance oil recovery (EOR).

ACKNOWLEDGMENT

I would like to express my sincere thanks to Dr. Xingru Wu, for his guidance and support in completing and conducting this research. It was a pleasure and an honor to work with Him.

I would also like to thank Prof David Ogbe and Dr. Akeem Akintola for their help as members of my committee.

My deepest gratitude to my parents Alhaji Yau Kaita and Safiya Ahmed Saee, my brothers Ahmed and Sadiq Yau Kaita who always supported my choices; I would not stand where I am without them.

I would also like to thank Isah Mohammed, for his unconditional support and advice. Without him, I could never have completed this research.

Dr. Alpheus Ibokoyi, Dr. Muktar Abdulrahman, Prof G K Falade and the rest of the faculty that taught me valuable petroleum engineering knowledge that I have used in this thesis and will use in my future life; my thanks go to them as well.

Thanks also to my colleagues and friends, who made my time at AUST not only a time of learning but also an unforgettable experience.

I finally want to extend my gratitude to the Petroleum Tax Development Fund (PTDF), for their sponsorship throughout the master's degree at AUST.

DEDICATION

This effort is dedicated to my fiancée (Hadiza Kado Danfuloti) for her patience, understanding, and encouragement in preparing this thesis.

TABLE OF CONTENTS

LIST OF FIGURES

LIST OF TABLES

CHAPTER ONE

INTRODUCTION

One of the major problems of developing a sour reservoir is how to handle the produced sour/acid gas. The gases produced from a sour reservoir are sweetened to selectively separate the gases using different methods . Among these methods, amine extraction is the most commonly used in petroleum industries. The separation process results in the production of a waste stream containing CO_2 and H_2S, and this mixture is referred to as acid gas. There is a need for an environmentally-friendly and cost-effective method for dealing with this acid gas stream.

Over the years a lot of strategies have been developed to handle acid gas mixture, and most of them are primarily concerned with the reduction of the toxic hydrogen sulfide to an inert/non-toxic reactive product. The most common technique is the Claus reaction process where gases containing H_2S are catalytically converted to elemental sulfur (Bennion et al. 1999)Another method used to manage the acid gas mixture is to inject a compressed acid gas mixture into a subsurface reservoir for storage.

In this research, I studied the re-injection of the rich waste acid gas stream directly back into the producing or depleted light oil reservoir for the purpose of miscible flooding enhanced oil recovery through characterizing its phase behavior and numerical simulation. Sour gas injection for enhanced oil recovery (EOR) presents a cost-effective and environmentally-friendly solution for managing a sour reservoir. It eliminates current taxation or future liability associated with emission or surface storage of sulfur. This study will focus on mechanisms of miscible gas injection using sour gas. Sour gas is a blend of natural gas with hydrogen sulfide (H_2S) and carbon dioxide (CO_2)

1.1 Research aim

The main goal of this research is to develop a miscible gas flooding EOR with sour gas using a compositional simulator with the aim to study the mechanism of how sour/acid gas enhances oil recovery and to understand how hydrocarbon composition in sour gas affects miscibility development and the minimum miscibility pressure.

1.2 Research objectives

To conduct minimum miscibility pressure (MMP) studies with a compositional variation of methane in the injected sour gas to determine how methane concentration affects the MMP of sour gas and its phase behavior.

Develop a compositional simulation model for the sour gas injection process and conduct sensitivity studies to determine the effect of some parameters on oil recovery efficiency.

1.3 Research Layout

This research is organized into four chapters. A brief introduction to the problem, objectives, and scope of the work are presented in Chapter One. Chapter Two contains a review of the published literature and a summary of related previous studies. This chapter also focuses on the miscible gas flooding EOR process, different gases used for gas flooding, miscibility development and methods used in determining minimum miscibility pressure and work done on sour gas injection. Chapter Three the base case model is presented. Chapter Four discusses the results obtained from the simulations, sensitivity studies, and comparative MMP studies, as well as the summary of the analysis of results obtained. Finally, conclusions, and recommendations, are presented in Chapter Five.

CHAPTER TWO

LITERATURE REVIEW

2.1 Hydrocarbon Recovery

Hydrocarbon development is usually divided into three stages: Primary depletion, secondary recovery, and tertiary recovery. Primary depletion refers to the volume of hydrocarbon produced by the natural energy prevailing in the reservoir. Secondary recovery is usually used after reservoir pressure, and rate start declining, while tertiary recovery or enhanced oil recovery (EOR) is applied after secondary recovery has become uneconomical. The objective of EOR processes is to recover the remaining oil after the primary and/or secondary recovery mechanism.

2.1.1 Primary Recovery

Primary recovery process techniques use the reservoir natural energy to force hydrocarbons out of the reservoir. The recovery efficiency of primary depletion depends mainly on existing reservoir drive mechanisms. These forces in the reservoir either can act simultaneously or sequentially (Ogienagbon et al. 2016)

Primary recovery from oil reservoirs is influenced by reservoir rock properties, fluid properties, and geological heterogeneities. The primary oil recovery factors range from less than 10% to 40% or higher, while the remainder of the hydrocarbon is left behind in the reservoir (Satter, Iqbal, and Buchwalter 2008)

2.1.2 Secondary Recovery

Secondary recovery involves the introduction of artificial energy into the reservoir via one wellbore and production of oil and/or gas from another wellbore (Romero-Zeron 2012)Usually, secondary recovery includes the immiscible processes of water flooding and gas injection or gas-water combination floods, known as water alternating gas injection

(WAG), where slugs of water and gas are injected sequentially. Simultaneous injection of water and gas (SWAG) is also practiced, however the most common fluid injected is water because of its availability, low cost, and high specific gravity which facilitates injection (Satter, Iqbal, and Buchwalter 2008)

2.1.3 Tertiary Processes

Tertiary recovery processes refer to the application of methods that aim to recover oil beyond primary and secondary recovery. During tertiary oil recovery, other than conventional water, immiscible gas is injected into the formation to effectively boost oil production (Green and Willhite 1998)EOR is a broader idea that refers to the injection of fluids or energy not normally present in an oil reservoir to improve oil recovery that can be applied at any phase of oil recovery including primary, secondary, and tertiary recovery (Romero-Zeron, 2012).

Thus, EOR can be implemented as a tertiary process if it follows a water flooding or an immiscible gas injection. It may also be a secondary process if it follows primary recovery directly (Satter, Iqbal, and Buchwalter 2008)EOR refers to the recovery of oil through the injection of fluid sand energy not normally present in the reservoir (Lake 1989)(Green and Willhite 1998)

The ultimate goal of EOR processes is to increase the overall oil displacement efficiency, which is a function of microscopic and macroscopic displacement efficiency (Romero-Zeron, 2012). One of the mechanisms limiting primary and secondary recovery from completely sweeping the reservoir is trapping of oil on the pore scale (microscopic). Hydrocarbon trapping increases as oil saturation decreases due to an increase in capillary forces. This trapping is best expressed as a competition between viscous forces, which mobilize the oil, and capillary forces, which trap the oil (Larry Lake,1989).

$$N_{Tl}=\left\{\frac{\left[K\left(\nabla\Phi_l+g\,\Delta\rho\,\nabla D\right)\right]}{\sigma_{\square}}\right\}$$ ……. Equation 1

Where K=permeability (mD), $\nabla\Phi_l$ = gradient of the flow potential (Psi/ft) , g= gravitational force constant (ft/s) , $\Delta\rho$= Change in density $\sigma_{\square}$ = Interfacial Tension (dynes/cm) ∇D=Pore throat Size

2.2 Displacement of Fluid in a Reservoir

2.2.1 Sweep Efficiency

Microscopic efficiency refers to the displacement or mobilization of oil at the pore scale and measures the effectiveness of the displacing fluid in moving the oil at those places in the rock where the displacing fluid contacts the oil (Don W. Green, 1998)(Satter A et al., 2008)

Macroscopic or volumetric displacement efficiency refers to the effectiveness of the displacing fluid(s) in contacting the reservoir in a volumetric sense (Romero-Zeron, 2012). Volumetric displacement efficiency also known as conformance, indicates the effectiveness of the displacing fluid in sweeping out the volume of a reservoir, both areal and vertically, as well as how effectively the displacing fluid moves the displaced oil toward production wells (Don W. Green, 1998).

The overall displacement efficiency of any oil recovery displacement process can be increased by improving the mobility ratio or by increasing the capillary number or both (Satter A et al., 2008).

$$E=E_v E_D$$ …… Eqn 1

$$E_V=E_L E_A$$ ……Eqn 2

Where, E = overall hydrocarbon displacement efficiency, E_v = macroscopic displacement efficiency E_L= vertical sweep efficiency, E_D = microscopic displacement efficiency and E_A = areal sweep efficiency

2.2.2 Effect of Capillary Number on Residual Oil Recovery

According to S, Thomas, capillary number represents the relative effect of viscous forces versus surface tension acting across an interface between two immiscible liquids. It is usually denoted N_c in the oil field. Mathematically, the capillary number is defined as:

$$N_c = \frac{v\mu}{\sigma Cos\theta} \quad \text{.....Eqn 3}$$

Where $v\mu$ represent the viscous force and $\sigma cos\theta$ represent the capillary force in the pore space. μ = Displacing fluid viscosity, v =Darcy's velocity and σ =Interfacial tension (IFT) between the displaced and the displacing fluids.

Figure 1 shows how the degree of trapping increases with a decrease in residual oil saturation. For a flowing liquid, if $N_T >> 1$, then viscous forces dominate over interfacial forces; however, if $N_T << 1$, then viscous forces are negligible compared with interfacial forces and the flow in porous media is dominated by capillary forces.

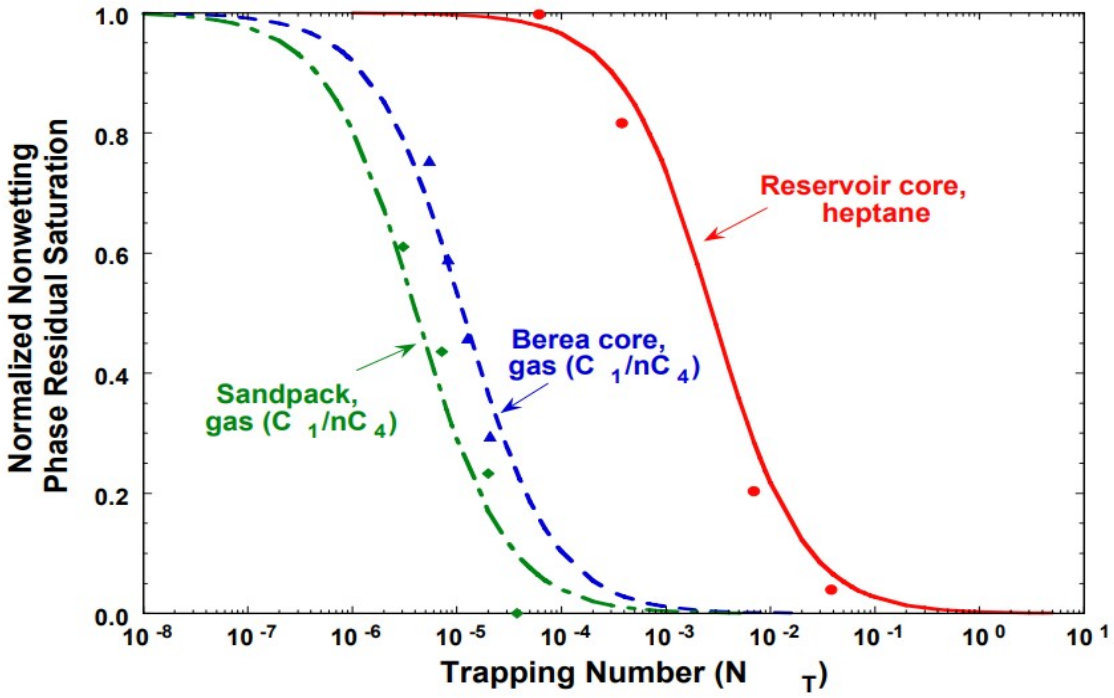

Figure 1: Comparison Model with Experimental Non-wetting Phase Residual Saturation (Pope 2007)

However, capillary numbers are usually large for high-speed flows and low for low-speed flows; thus, typically for flow through pores in the reservoir $N_c \sim 10^{-6}$, and for flow in production tubular $N_c \sim 1$.

The Capillary number in a miscible displacement becomes infinite, and under such conditions, residual oil saturation in the swept zone can be reduced to zero if the mobility ratio is “favorable”.

2.2.3 Mobility-control processes

Fluid mobility (λ_i) is defined as the ratio of the fluid effective permeability to its viscosity, and the mobility ratio (M) is defined as the ratio of the mobility of the displacing phase (λ_D) to the mobility of the displaced phase (λ_d). Mobility control processes are used to describe any process where an attempt is made to alter the relative rates at which injected and displaced fluids move through a reservoir (Green and Willhite 1998)

$$\lambda_i = \frac{K_i}{\mu_i} \quad \text{…… Eqn 4}$$

$$M = \frac{\lambda_D}{\lambda_d} \quad \text{……...Eqn 5}$$

High mobility ratios result in a poor displacement and low sweep efficiencies, which can be caused by a large viscosity contrast between the displacing fluid (i.e. water) and oil (Lyons and Plisga 2005)

The overriding of the displaced phase by the displacing phase eventually develops into phase trapping. While this is a major challenge in secondary recovery schemes like water flooding, chemical flooding can be used to prevent this phenomenon by adjusting the capillary and viscous forces in-situ media so that the displacement process is favored. The process can be attained by either increasing the viscosity alone or reducing the capillary pressure simultaneously as demonstrated in the application of multiple Chemical EOR agent at a time. The process has proven to be effective in increasing recovery and reducing residual oil saturation when a dimensionless ratio called capillary number is increased.

2.3 Mechanism of Gas Flooding in EOR

Gas flooding refers to those EOR techniques whose main oil recovery mechanisms include extraction, vaporization, solubilization, and condensation. However, some of the injectants such as CO_2 possess other, important oil recovery mechanisms such as oil viscosity reduction, oil swelling, and solution gas drive. Most of the gas injection processes can be categorized as either miscible or immiscible.

The immiscible gas flood increases oil recovery by raising the capillary number due to the relatively low interfacial tension values between the oil and injected gas and high reservoir pressure. In miscible flooding, the incremental oil recovery is obtained by one of the three

mechanisms: oil displacement by solvent through the generation of miscibility (i.e., zero interfacial tension between oil and solvent–therefore infinite capillary number), oil swelling and reduction in oil viscosity

Miscible flooding can be used with or without water for the control of viscous fingering and the reduction in gas-oil interfacial tension of the system. Miscibility is achieved by re-pressurization to bring the reservoir pressure above the MMP of the fluids.

Christensen et al. observed that it is difficult to distinguish between miscible and immiscible processes since in many cases multi-contact gas-oil miscibility may have been obtained. This leads to uncertainty about the actual displacement process. Loss of injectivity and/or failure of pressure maintenance in the actual reservoir, attributable to many factors, cause the process to fluctuate between miscible and immiscible during the life of the process.

Gas injection has been reported to be the most successful method for EOR in light, condensate and volatile oil reservoirs (Rahmatabadi 2011)(Hinderaker et al. 1996)

Continuous efforts are being made to improve the flood profile control in gas flooding. These include the preparation of direct thickeners with gas-soluble chemicals like telechelic Disulfate, Polyflouroacrylate and fluoroacrylate-styrene copolymers, which can increase the viscosity of gases several folds (Moritis 1995)

2.3.1 Types of Gas Injection

Gas can be injected and flood the reservoir in a miscible or immiscible way. Depending on the location of the gas injection the flooding can be crestal injection or pattern injection. For the crestal gas injection, the injection-well is usually placed in higher structural position so that the gravity difference between the oil and gas can be used to stabilize the displacement front. This manner of injection is generally used in reservoirs with significant structural relief or thick oil columns with good vertical permeability.

Alternatively, for other types of reservoirs without structural relief or high vertical permeability, pattern gas injection consists of a geometric arrangement of injection wells for uniformly distributing the injected gas throughout the oil-productive portions of the reservoir. In practice, injection-well/production-well arrays often vary from the conventional regular pattern configurations, e.g. five-spot, seven-spot, nine-spot to irregular injection-well spacing (Green & Willhite, 1998).

The selection of an injection arrangement is a function of reservoir structure, sand continuity, permeability and porosity levels and variations, and the number and relative locations of existing wells (Cotter 1962) There are several limitations to pattern-type gas injection. Little or no improvement in recovery is derived from a structural position or gravity drainage because both injection and production wells are located in all areas of the reservoir. Low areal sweep efficiency results from gas override in thin stringers and by viscous fingering of gas caused by high flow velocities and adverse mobility ratios (Ahmed and McKinney 2005)

Typical results of applying pattern injection in low-dip reservoirs (Shehabi, 1979) rapid gas breakthrough, high producing GORs, significant gas compression costs to reinject the gas into the reservoir.

Miscible gas injection implies that the displacing gas is miscible with reservoir oil either at first contact or after multiple contacts. A transition zone will develop between the reservoir oil and displacing gas. Mechanisms of miscible gas flooding include reduction of oil viscosity, the vaporization of oil, and the reduction of interfacial tension.

Miscibility is the mixing of multiple substances in all proportions and creates a homogeneous phase without the existence of an interface between them (Holm 1986)

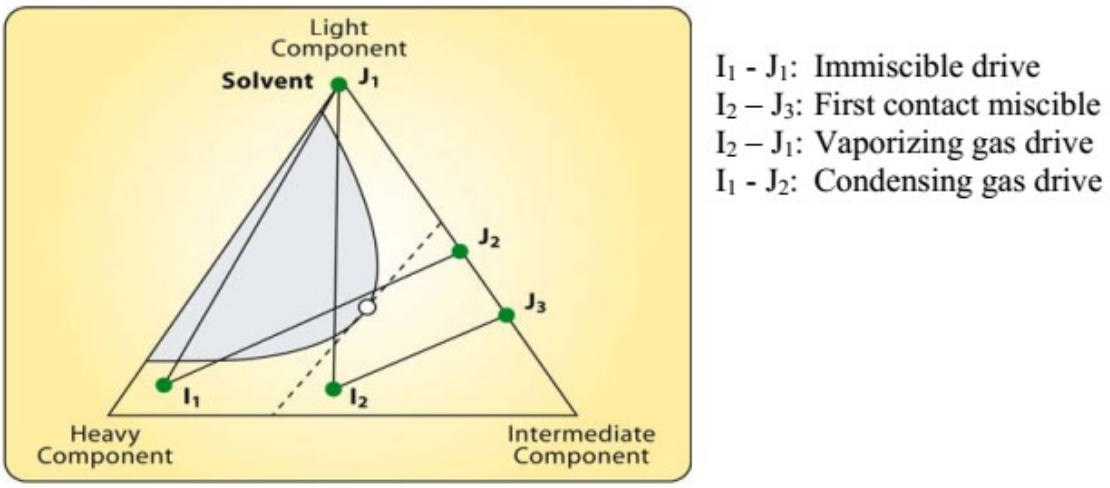

Figure 2: Conditions for different types of oil displacement by solvents(Lake L. W., 1989)

The successful design and implementation of a miscible gas injection project depends upon the accurate determination of the MMP and other factors such as reservoir and fluid characterization. The MMP indicates the lowest pressure at which the displacement process becomes a multiple-contact miscible (Lake L. W., 1989). Miscibility can be achieved either first contact miscibility or multi-contact miscibility as shown in Figure 2.

First contact miscibility occurs when two fluids immediately form a single phase regardless of fluid proportions. Liquefiable petroleum gas (LPG) or low molecular weight hydrocarbons such as ethane, propane, and butane are the most common solvent used for first contact miscible flooding.

The basic requirement for slug injection is that the solvent slug must be miscible with both the reservoir oil and the drive gas, which is usually lean gas.Figure.3 illustrates the phase behavior requirements for first contact miscibility at both the leading and trailing edges of an LPG slug (Rahmatabadi 2011)

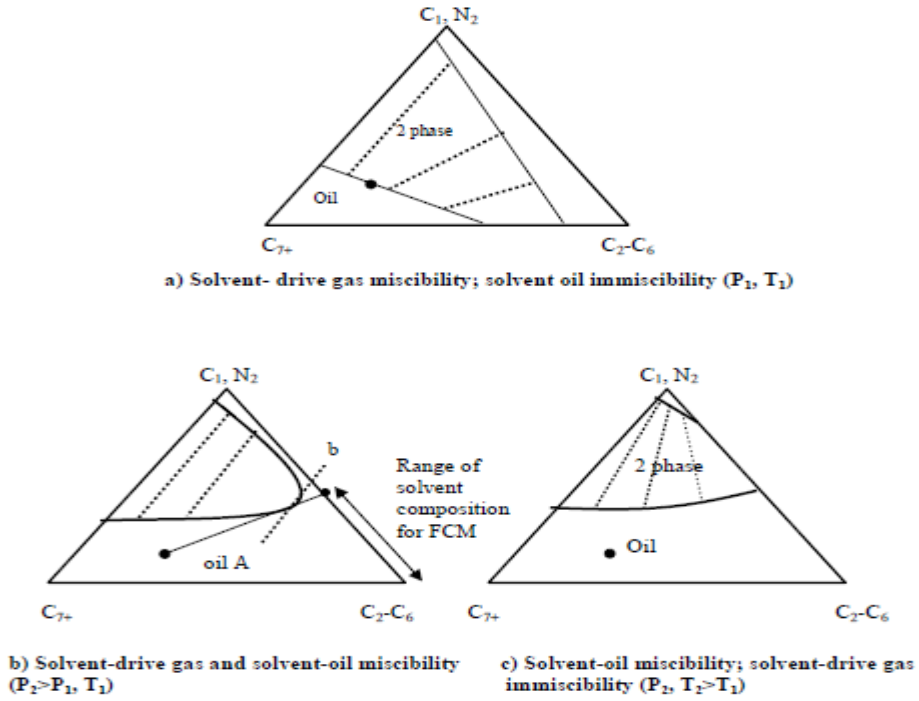

Figure 3: First Contact Miscibility in Pseudo-ternary Diagram (Stalkup 1987)

In terms of ternary diagrams, the gas composition located on the critical tie line passing through the oil composition is the leanest composition that can provide first contact miscibility (FCM) with the oil at the specified pressure and temperature of the ternary system. The pressure of the ternary system is the CMP corresponding to that composition.

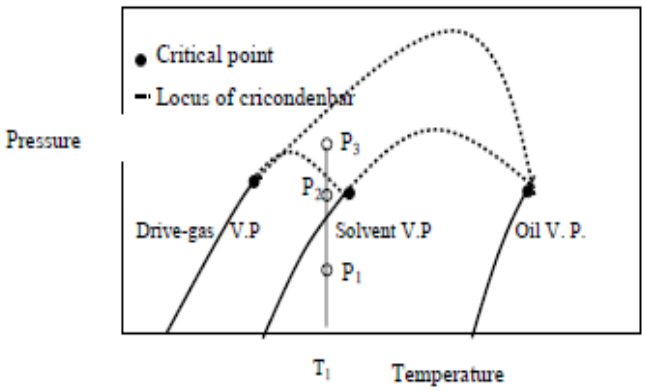

Figure 4: Phase Behavior Consideration For first Contact Miscibility (Stalkup 1987)

For multiple-contact miscibility (MCM), the miscibility is developed miscibility through mass transfer as gas moves along in the porous medium and contacts fresh oil. In developing MCM, the transfer of components between the two phases is essential and is facilitated by the flow of phases in the porous medium. MCM can happen in three types of displacements: a vaporizing gas drive, a condensing gas drive, and a condensing/vaporizing (CV) drive (Stalkup 1987)

In a vaporizing gas drive, gas contacts fresh oil at the front of the displacement. Some of the intermediate components of the oil are vaporized to gas, thus enriching the gas. The enriched-gas moves along and contacts fresh oil at the front, and the new contacts further enrich the gas. Within a finite number of contacts, the gas may be sufficiently enriched to develop miscibility with fresh oil (Rahmatabadi 2011)

In a condensing gas drive (or enriched-gas drive), the gas is relatively enriched with intermediate components while the oil is relatively heavy. When gas first contacts the oil, some intermediate components condense from the gas to the oil, resulting in lighter oil. This lighter and enriched oil does not move as fast therefore is left behind and contacted by fresh gas. As a result, the enriched oil becomes further enriched, and after repeated contacts, the oil is sufficiently enriched to be miscible with the fresh gas (Rahmatabadi 2011)

The condensing/vaporizing gas drive, first described by Zick and Stalkup, shows that another mechanism may develop from injection of enriched-gas without necessarily achieving a miscible condition. The combined condensing/vaporizing mechanism they describe is a process that exhibits a sharp near-miscible “front.”

A condensing mechanism occurs just ahead of the front, and a vaporizing mechanism trails the front. A practical consequence of this mechanism is that a lower enrichment level can be

used for the injection gas than would be estimated from the traditional interpretation of the enriched-gas miscible drive process (Rahmatabadi 2011)

2.3.2 Type of Gases Used in Gas Flooding

In the earliest applications of gas injection, both liquefied petroleum gas (LPG) and lean hydrocarbon gases constituted the major share of injectants for gas injection EOR. However, this process became economically unattractive with increasing natural gas prices. It gives rise to the use of other gases that are cheaper or waste products such as CO_2, N_2 Flue gas, sour gas Etc.

CO_2-EOR has been successfully implemented in both mature and water flooded carbonate reservoirs (Moritis 2008)$_2$ flooding from natural sources has been the most important EOR process in the U.S. and particularly in carbonate reservoirs of the Permian Basin. (Moritis 2008)$_2$ floods in the U.S. being 63 projects in carbonate formations mainly in the Permian basin of Texas.

N_2 flooding has been an effective recovery process for deep, high pressure, and light oil reservoirs. Generally, for these types of reservoirs, N_2 flooding can reach miscible conditions. However, immiscible N_2 injection has also been used for pressure maintenance, cycling of condensate reservoirs, and as a drive gas for miscible slugs (Manrique et al. 2007) High capital (e.g., Air separation units) and operational (e.g., N_2 rejection units, if required) costs associated to N_2 injection have reduced the interest in this recovery process in recent years. Though, N_2 injection still represents an option that can be justified for high pressure and high temperature (HP/HT) light oil reservoir if there is no access to other gas sources (Linderman et al. 2008)

Al-Hadhrami et al. developed a sour gas flooding process for a reservoir contained by carbonate stringers in Oman. They develop the process in phases based on the production data, logging result, and appraisal drilling information. The interference test shows that there is a pressure communication across the field which eliminated the risk of reservoir compartmentalization, it also showed that there is no single high permeability zone between one well to another. They further carried out a sensitivity analysis on different injection gas composition, the result showed that rich hydrocarbon attains miscibility at a lower pressure than lean hydrocarbon gas hence the higher recovery for rich hydrocarbon gas. CO_2 gives the highest recovery factor at 1.0 hydrocarbon pore volume (HCPV) injection, while N_2 has the lowest recovery factor because it required higher pressure to achieve miscibility. The result was based on average minimum miscibility pressure of about 38MPa.

Figure 5 shows the overall recovery achieved using different gas at 1 HCPV injection at the average MMP.

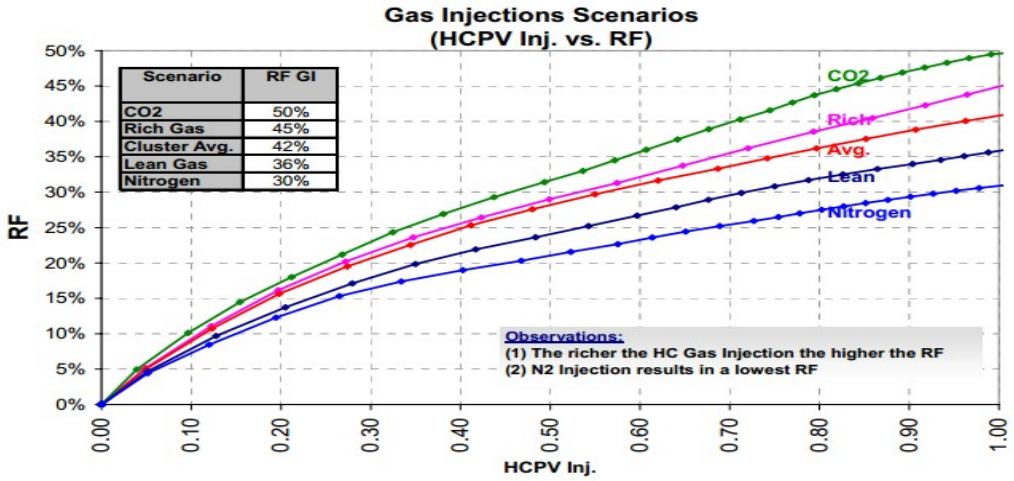

Figure 5: Gas Injection Scenarios (Al-Hadhrami et al. 2007)

2.4 Determination of Minimum Miscibility Pressure (MMP)

MMP is the lowest pressure at which oil and gas develop miscibility at a fixed temperature. It is the key parameter in designing miscible gas injection, MMP can be determined experimentally or computationally.

2.4.1 Experimental Methods for Estimating MMP

MMP can be estimated through a number of experiments: slim-tube experiments, mixing-cell experiments, rising bubble/falling drop experiments, and vanishing interfacial tension experiments.

The slim-tube experiment is the most widely accepted experimental method for estimating MMP. A slim-tube is a long, narrow tube packed with glass beads or sand. The length of the tube is between 5 and 120 ft (Orr et al. 1982)(Elsharkawy et al. 1992)

The injection temperature and pressure are kept constant (pressure is generally kept constant by a back-pressure regulator). The rate of gas injection is such that it does not induce a large pressure gradient. The slim-tube displacement velocity is typically between 120 and 200 ft/D (Danesh 2007)

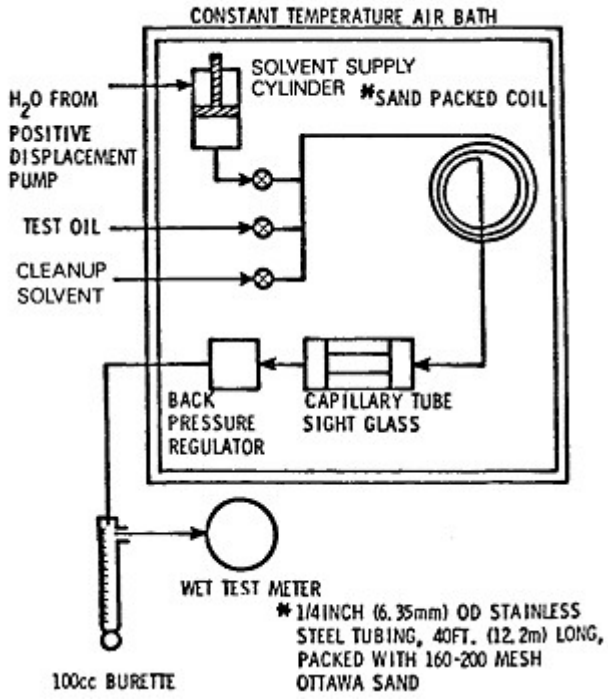

Figure 6: Schematics diagram of Slim-tube apparatus (Yellig and Metcalfe 1980)

To determine MMP, three or more slim-tube experiments were performed. In each experiment, oil recovery and pore volume of injected gas were recorded. The recovery data was then used to estimate MMP using a number of criteria. The most common criterion is the break-over pressure in a plot of recovery versus pressure when recovery is recorded after typically injecting 1.2 pore volume of gas (Yellig and Metcalfe 1980)(Holm and Josendal 1974)(Hudgins et al. 1990)

Slim-tube experiments, however, have significant drawbacks. These drawbacks partly come from the lack of standards both in conducting the test and in interpreting its results. (Elsharkawy et al. 1992)

Furthermore, the results of a slim-tube experiment can be uncertain because of the lack of data points and because of the impact of dispersion (Johns et al. 2002)

Multiple-contact experiments can accurately estimate MMP under certain conditions. The main purpose of a multiple-contact test is to study the phase behavior of injection gas and oil (Menzie and Nielsen 1963)

The multiple-contact test relies on contacts between oil and gas. In each contact, oil and gas are mixed at a specified ratio in a pressure-volume-temperature (PVT) cell and brought to equilibrium. A single PVT cell or a series of cells is used to make repeated contacts between oil and gas in a forward or a backward manner.

The main drawback of multiple-contact tests is their inability to measure MMP for a condensing/vaporizing drive. These experiments can be a fast and cheap alternative to slim-tube experiments when the miscibility mechanism is known beforehand to be either condensing or vaporizing (Rahmatabadi 2011)

Rising bubble apparatus (RBA), first proposed by (Christiansen and Kim)(Christiansen and Kim)

Although it is fast and cheaper as compared to slim-tube experiments, the rising bubble method has a significant drawback, the primary of which is its unreliability in predicting MMP for condensing and condensing/vaporizing gas drives. The rising gas bubble attempts to duplicate the forward contact of gas and oil in reservoirs. As gas rises, it makes contact with fresh oil at any stage of the experiment.

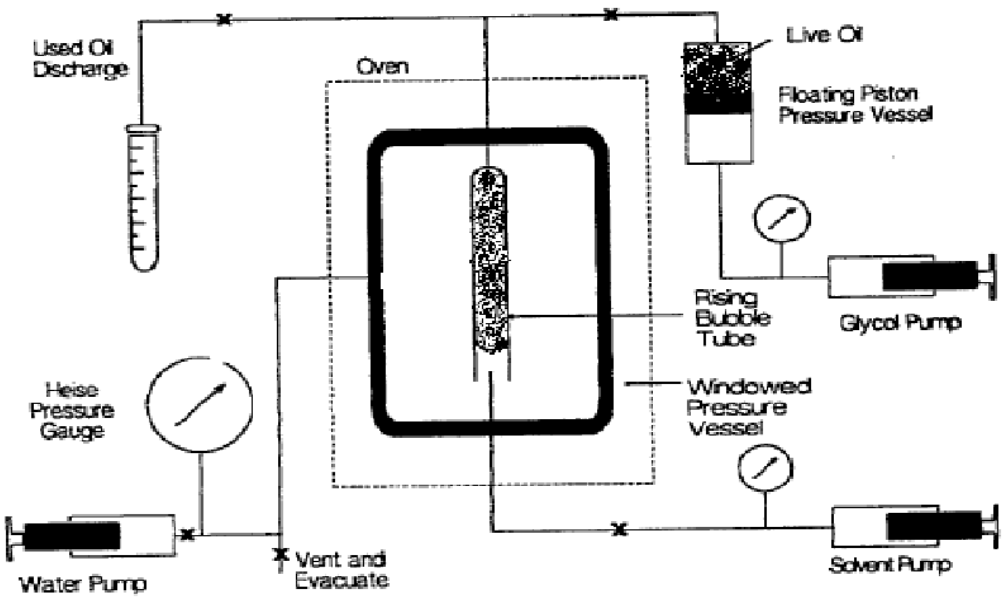

Figure 7: Schematic diagram of rising bubble apparatus (Eakin and Mitch 1988)

As a result, the gas becomes richer and richer as it gets closer to the top, similar to the advancing gas front in the reservoir, but not necessarily the same. If miscibility develops, therefore, it will do so at the front of the advancing gas. Thus, rising bubble experiments can likely predict the MMP for a vaporizing gas drive, but not for a condensing drive (Zhou and Orr 1998)

The falling drop experiment is a modified version of the rising bubble experiment and was used for predicting MME (Christiansen 1986; Zhou and Orr 1998) and MMP in a condensing gas drive. The mechanism of the experiment is the same as the rising bubble, the difference being that a bubble of oil is introduced into a gas-filled chamber. As with the rising bubble experiment, it is unclear whether the falling drop method can accurately predict the MMP for a vaporizing/condensing gas drive, and therefore it is not commonly used in the industry (Zhou and Orr 1998).

2.4.2 Empirical Correlations

Multiple-contact miscible floods have proven to be one of the most effective enhanced oil recovery methods currently available (Iman and Mahmood 2012)(Metcalfe et al. 1973)(Iman and Mahmood 2012)

Kovarik developed a correlation to determine the MMP of impure CO_2 by using the mole fraction rule to determine the pseudocritical temperature. He found that the weight average fraction properties correlated with the data similar to the mole average fraction properties.

$$MMP_{impure\,CO2} = 0.2814\left[548 - \left(1.8\,T_{pc} + 492\right)\right] + MMP_{pure\,CO2} \quad \text{..... Eqn 7}$$

Where

$$T_{pc}=\sum_{i=1}^{n} x_i T_{ci}$$ ……. Eqn 8

X_i = Component mole fraction

T_{ci} = Component critical temperature

Kovarik correlation has some limitation, it is used only for C_1 as a non-CO_2 component with less than 20 mol% ratios. It can only be used to predict pure and impure CO_2 MMP.

Eakin and Mitch developed their correlation injected gas pseudocritical pressure. They stated that the change in the rising bubbles in the rising bubble apparatus and the low value of the interfacial tension between the injected gas and oil would occur only near the critical point. However, they didn't consider the presence of some non-CO_2 component such as SO_2 and O_2.

$$\ln_{Pr,impure\ CO2}=\left(0.1697-\frac{0.06912}{T_r}\right)y_{C1}\left(\sqrt{MW_{C7+}}\right)+\left[2.3855-\frac{0.005955\left(MW_{C7+}\right)}{T_r}\right]y_{C2+}+\left(0.1776-\frac{0.01023}{T_r}\right)y_{N2}\left(\sqrt{M}\right.$$

…….Eqn 9

Where

$$p_{r,impure\,CO2}=\frac{MMP_{impureCO2}}{P_{Cm}},$$ ……..Eqn 10

$$P_{cm}=\sum_{i=1}^{n} x_i P_{ci}$$ ……Eqn 11

$$T_r=\frac{1.8T_r+492}{1.8T_{CM}+492}$$ ……...Eqn 12

$$T_{CM}=\sum_{i=1}^{n} x_i T_{ci}$$ ……Eqn 13

X_i = Component mole fraction, T_{ci} = Component critical temperature, P_{ci}=Component critical pressure

Glaso Correlation

Glaso proposed a correlation for predicting MMP of multi-contact miscible displacement of reservoir fluid by hydrocarbon gases, N_2 and CO_2. The correlation gave the MMP as a function of reservoir temperature, molecular weight of $C_{7+,}$ mole percent ethane in the injection gas and the molecular weight of the intermediates (C_2 through C_6) in the gas. The proposed equations by Glaso are as follows:

$$MMP = 6{,}329 - 25.410y - (46.475 - 0.185y)z + (1.127 \times 10^{-12} y^{5.258} x e^{319.8z\, y^{-1.703}})T \quad \text{……Equation 14}$$

Where, *x*= is the molecular weight of C_2 through C_6 components in injection gas, in lbm/mol, *y*= is corrected molecular weight of C_{7+} in the stock-tank oil in lbm/mole and T = Reservoir temperature

$$y = \frac{\gamma_{oC7+}^{-0.846}}{2.622^{6.558}} \quad \text{……..,,…….. Eqn 15}$$

ɣ = specific gravity of heptane-plus fraction, and z = mole percent methane in injection gas

Firoozabadi et al. Correlation

A simple correlation proposed by Firoozabadi and Khalid predicted MMP of reservoir fluids using lean natural gas or N_2 for injection. Three parameters accounted for the effect of multiple-contact miscibility of a reservoir fluid under N_2 or lean gas flooding: The concentration of intermediates, the volatility, and the temperature. The correlating parameters included the ratio of the intermediates (mole percent) divided by the molecular weight of the C_{7+} fraction. Intermediates contents of a reservoir fluid are usually attributed to the presence of C_2 through C_6, $CO_{2,}$ and H_2S.

Firoozabadi and Khalid observed that exclusion of C_2 from intermediates improves the correlation of the MMP. Therefore, intermediates in this study are defined by C_2 through C_5 and CO_2 components. The heptane-plus molecular weight indicate the oil volatility. The equation is as follows:

$$MMP = 9433 - 188\,x\,10^{3}\,\frac{xint^{2}}{\square}\,\frac{M_{C7+T^{0.25}}}{xint}\,\square\,\dot{\iota}\,M_{C7+T^{0.25}} \quad \text{Eqn 16}$$

Where

MMP = Minimum Miscibility Pressure (Psi), x_{int} = mole percent intermediate in reservoir oil (C_2-C_5 and CO_2), T= reservoir temperature and M_{C7+} = molecular weight of heptane-plus

2.4.3 Thermodynamic Method

In this method, selected EoS is calibrated to experimental PVT data including swelling and slim-tube measurements. Using reliable experimental data in tuning EoS makes EoS methods the most reliable prediction methods (Iman and Mahmood 2012)

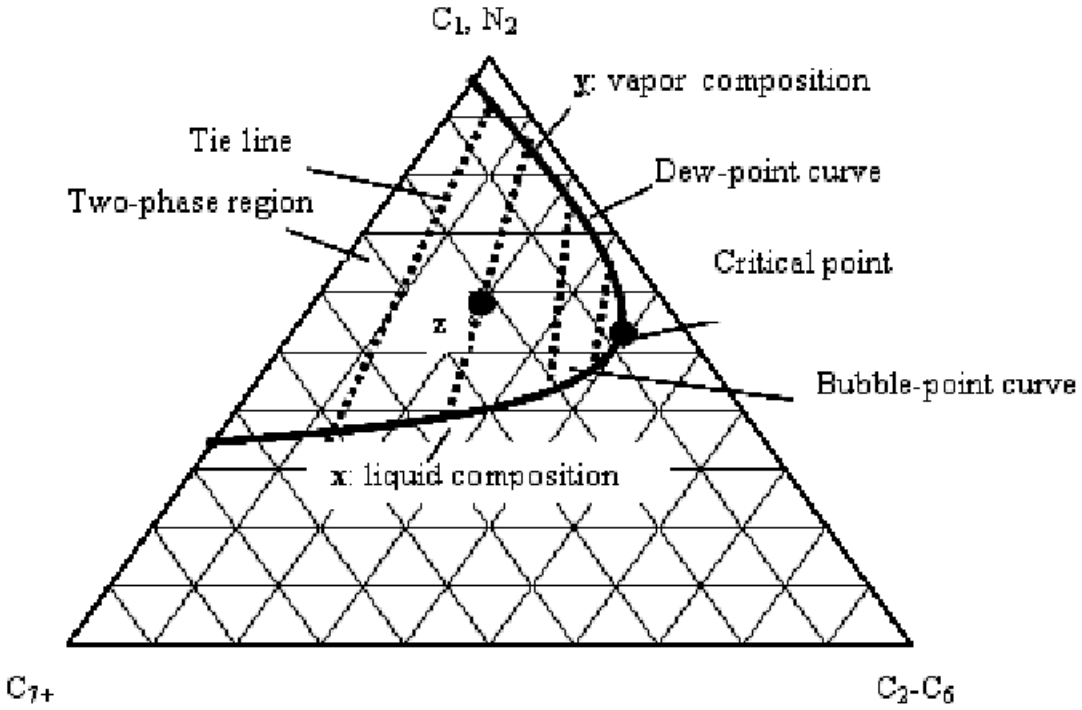

Figure 8: Ternary diagram at a specific temperature and pressure

In this method, the MMP is explained traditionally by ternary diagrams. The limiting tie line is the extension of the tie line passing through the composition of the original oil, and the tie line which passes through the critical point of the ternary diagram is called a critical tie line. Monroe et al., showed three key tie lines which control displacement behavior in the reservoir: The tie lines that extend through injection gas composition, the tie line passing through the oil composition, and the third tie line called "the crossover tie line." Multi-contact miscibility occurs if any of these tie lines correspond to the critical tie line.

In vaporizing gas drive mechanisms, miscibility is controlled only by the limiting tie line passing through the oil composition and is not dependent on injection gas composition. The gas phase composition varies along the dew-point phase boundary expressed at constant pressure and temperature in pseudo-ternary diagrams towards the critical point composition.

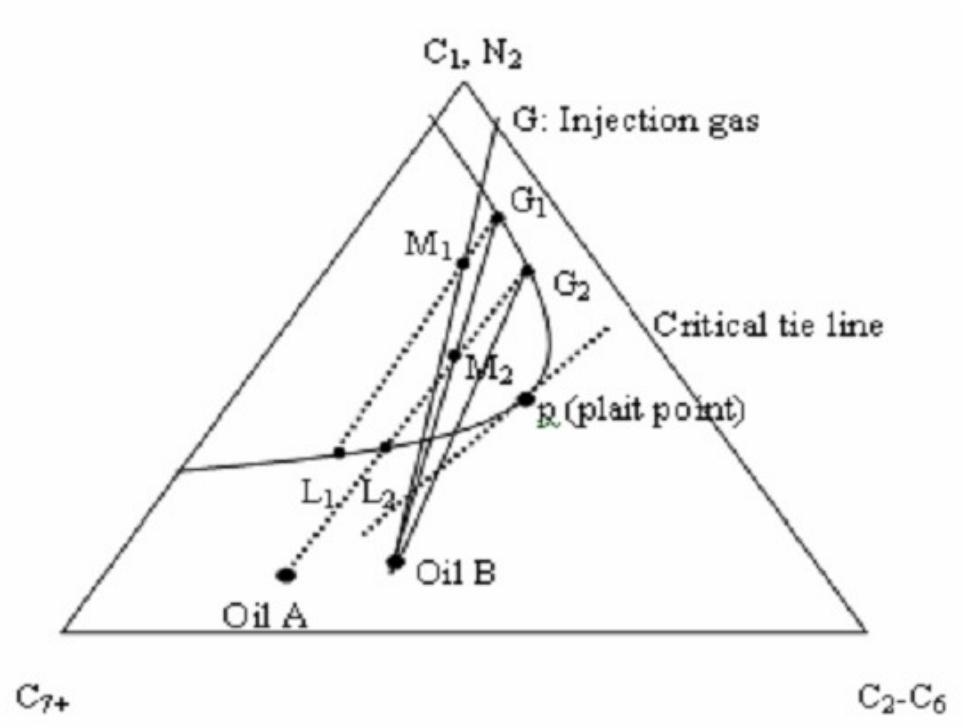

Figure 9: Vaporizing-gas drive mechanism (Stalkup, 1987)

In condensing drive mechanisms, the key tie line passing through the injection gas composition controls the development of miscibility. In this displacement, mechanism miscibility is obtained at the site of injection. The intermediate components are condensed from the injection gas to the reservoir oil and miscibility develops as the tie line passing through the injection gas composition becomes the critical tie line expressed in the ternary diagram model. Orr and Silva showed that crossover tie line controls the development of miscibility in combined vaporizing-condensing mechanisms.

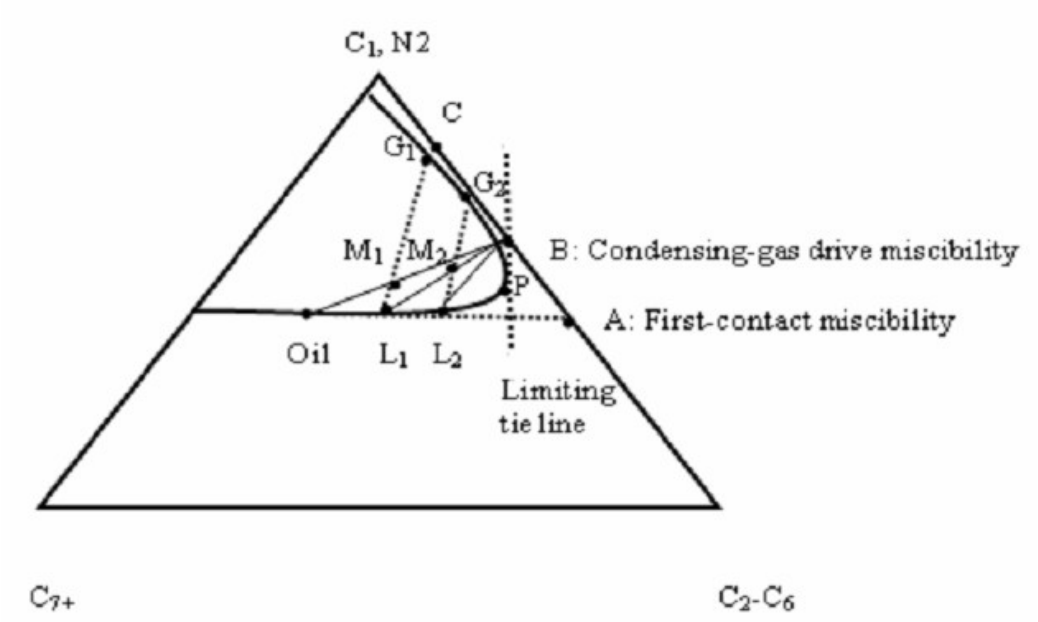

Figure 10: Condensing-gas drive mechanism (Stalkup, 1987)

2.5 Sour gas Injection

Natural gas is considered sour if there are more than 5.7mg of H_2S per cubic meter of natural gas, which is equivalent to approximately 4ppm by volume under standard temperature and pressure according to the Texas Commission on Environmental Quality (TCEQ). Sour natural gas is produced as either free gas or as a liberated solution gas from sour oil.

Van Vark et al. evaluated the feasibility of large-scale injection of sour and acid gas into low permeable carbonate reservoir to enhance oil recovery. They considered lean gas, sour gas and acid gas to evaluate the ultimate recovery achieved by different gases. Their results showed that lean gas plateau takes about 2.5% of STOIIP per year and is sustained for about ten years after which the gas breaks through, resulting in a rapid GOR increase. Sour gas yields similar production profile as lean gas but the latter displaces in a more stable rate, resulting in a 25% longer plateau. After the gas breakthrough, the oil rate declines similarly. Acid injection has a lower plateau rate due to high viscosity but lasts longer and ultimately results in a higher recovery factor.

Khan et al. examined the strategies to maximize the enhanced gas recovery in a natural gas reservoir via subsurface storage of potentially associated waste gases such as CO_2 and H_2S. The simulation results showed that additional gas is recovered by gas-displacement after injecting CO_2 and acid gas (CO_2– H_2S) in two separate scenarios. An early breakthrough was observed when pure CO_2 was injected. For acid gas, it took a little bit longer before the gas breaks through in the production well consequently increasing the ultimate recovery of the field.

Haynes et al. presented a development approach for injecting sour gas in a carbonate reservoir of a field in South Oman. They injected the gas in stages, with different CO_2 and H_2S composition; it began with a composition of 1.93 mol% H_2S and 4.05 mol% CO_2, a make-up sweet gas for voidage replacement of below 1 mol% CO_2 and H_2S. It was then increased to 3.04 mol% H_2S and 10.72% CO_2 and stopped the sweet gas make-up. This increased the recovery factor by about 15%.

Chen et al. optimized the injection and production parameters for sour gas storage underground for a gas reservoir in Ordos Basin. They used the numerical method to study the movement mechanism of H_2S and the effect of some parameters on H_2S mole fraction in the produced gas. Some of the parameters they looked at were ultimate recovery factor, injection rate, production rate, and injection-production cycle. The sensitivity analysis result showed that H_2S mole fraction in produced gas decreases as the injection-production cycle number increases. In addition, it showed that the H_2S mole fraction produced depends heavily on ultimate recovery factor, injection rate, production, and the rate ratio.

Bennion et al. developed screening criteria for selection of zones suitable for acid/sour gas re-injection or disposal in a reservoir, and highlights potential areas of concern for reduced injectivity. Due to acid gas induced formation dissolution, fines migration, precipitation, and

scale potential, oil or condensate banking and plugging, asphaltene and elemental sulfur deposition, hydrate plugging and multiphase flow phenomena associated with acid gas compression.

Chugh et al. developed an acid gas injection strategy into a sour gas reservoir as an alternative to building a new large sulfur plant where production and injection will occur concurrently. They used a compositional numerical simulator to forecast production rate under concurrent production and injection scenarios. They also modeled an in-situ miscibility and gravity separation effect of acid gas and evaluated the risk associated with the operation to determine the optimal solution for it. From the result of the simulation, it showed that breakthrough is directly proportional to the injection rate. For high injection rate, gas breaks through in 12 years and low injection rate took about 25 years for gas to breakthrough. However, it should be noted that the study was done on a gas reservoir and breakthrough mechanisms may occur differently in an oil reservoir.

2.5.1 Reservoir Selection for Injection of Sour Gas

The specific location of the acid gas injection-well is based on a general assessment of the local and regional geology and hydrogeology, which is designed to evaluate the potential for leakage. Size and geometry of the injection zone, to determine that it is large enough to volumetrically hold all of the injected acid gas over the project lifetime. Thickness and extent of the overlying confining layer (cap rock), location and extent of the underlying or lateral bounding formations, folding, faulting, fracturing in the area, and an assessment of seismic (neotectonic) risk that may affect the containment of acid gas rate. Direction of the natural flow system, to assess the potential for migration of the injected acid gas permeability and heterogeneity of the injection zone and chemical composition of the formation fluids (water for aquifers, oil or gas for reservoirs) and formation temperature and pressure

To maintain supercritical fluid, bottom-hole injection temperature and pressure are conditioned such that the gas is miscible with the existing reservoir fluid. This is necessary to avoid adverse relative permeability effects due to the creation of immiscible liquid and vapor phase which can reduce the injectivity of the acid gas (Siddiqui et al. 2013)

$^{-6}$ mD (1 nanoDarcy) (Bennion et al., 1999)

2.5.2 Sour Gas Injection for EOR

Sour gas injection for enhancing oil recovery (EOR) is a viable option that presents a solution to many problems currently in the industry. It eliminates current taxation or future liability associated with emission or surface storage of sulfurThe improved performance relates to the increasing viscosity and higher density of the injected sour gas.

2.5.3 Sour Gas Phase Behavior

For an effective sour gas injection program, understanding the thermodynamic properties and phase behavior of the gas is necessary. Similarly, a good understanding of fluid phase behavior is equally important. The phase behavior of the acid gas binary system is represented by a continuous series of two-phase envelopes (separating the liquid and gas phases) located between the unary bounding systems in the pressure-temperature space (Carroll and Lui, 1997).

The properties of the acid gas mixture are important in facility design and operation. This is so because to optimize sequestration and minimize risk, the acid gas needs to be injected as a dense fluid phase to increase sequestration capacity and minimize buoyancy in order to meet reservoir pressure at a lower horsepower, at bottom-hole pressures greater than the formation pressure, for infectivity; at temperatures in the system generally greater than 35^{o}C to avoid hydrate formation, which could plug the pipelines and wellbore; and with water content lower than the saturation limit, to avoid corrosion.

Table 1: Properties of H_2S and CO_2 (Carroll, 2010)

Physical Property	H_2S	CO_2
Critical Temperature, K	373.5	304.2
Critical Pressure, MPa	8.963	7.382
Critical Volume. $m^3/kmol$	0.0985	0.0940
Critical Density, kg/m^3	346	468
Critical Compressibility, $(P_c V_c/RT_c)$	0.284	0.274
Triple Point Temperature, K	187.7	216.6
Triple Point Pressure, kPa	23.2	518
Normal Boiling Point, K	212.8	---
Melting Point, K	187.7	---
Specific Gravity Of Gas Relative to Air	1.177	1.520

An important aspect of the design of a sour gas injection scheme is the non-aqueous phase equilibrium. The binary mixture H_2S and CO_2 is the most important non-aqueous system involved in acid gas injection.

Bierlein and Kay measured vapor-liquid equilibrium (VLE) in the range of temperature from 0 °C to 100 °C and pressures to 9 MPa, and they established the critical locus for the binary mixture. For this binary system, the critical locus is continuous between the two pure component critical points. Sobocinski and Kurata confirmed much of the work of Bierlein and Kay$_2$S and CO_2 are completely miscible.

Robinson and Bailey$_2$S + CO_2. The points for the binary mixtures were at temperatures between 4°C and 71°C and at pressures from 4 to 8 MPa. Figure 8 shows the phase envelop for a binary mixture of H_2S and CO_2 the banana-shaped phase envelopes are characteristic of the acid gas mixture.

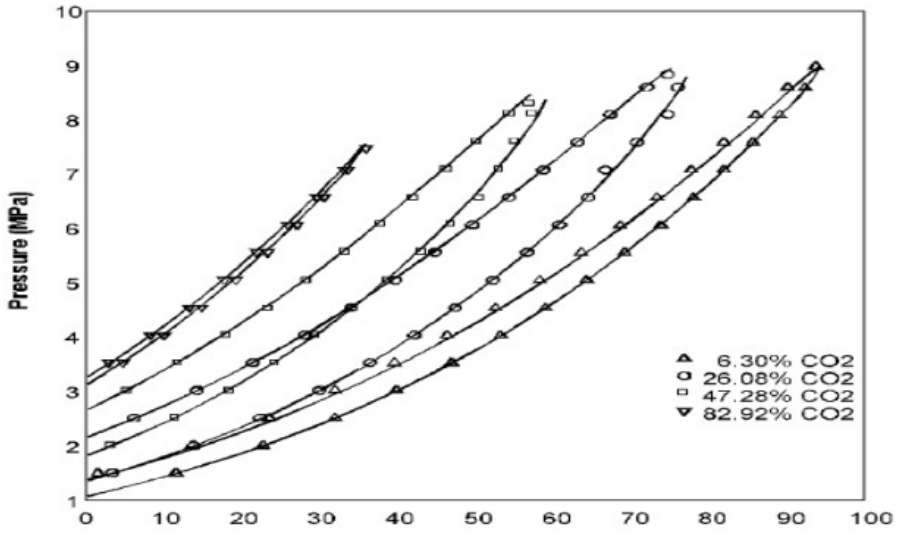

Figure 11: Phase Envelope For H_2S and CO_2 Mixture (Bierlein and Kay, 1953)

Effect of Acid gas on Thermodynamic/Chemical Equilibrium in the Fluid/Rock System

Ghoodjani and Bolouri discussed the benefit of CO_2 with respect to the acid gas effect on the rock, particularly in carbonates which tend to have faster reaction times when compared to sandstones. This is because, CO_2 reacts with the rock to form carbonic acid and more importantly when it is injected at high rates the permeability improves around the wellbore due to calcite minerals dissolution as a result of the acid effect.

Likewise, Ceragioli and Gianelli gave a comprehensive analysis of thermodynamic/chemical equilibrium involved when acid gas contacts carbonate reservoir rock containing connate brine and the fluid-rock interaction process associated. The experiment was conducted on a sour carbonate reservoir containing volatile oil at an isothermal condition of 100^{o}C. They used different possible injection gases with changing compositions ranging from that of the raw reservoir fluid (original mixture) to pure acid gas with 100% H_2S + CO_2 content.

Karim phase behavior examination showed that acid gas could exhibit a liquid-like behavior because its density increases under supercritical conditions at higher pressures. In some cases, they may become even denser than the volatile reservoir fluid to be produced.

Additionally, he stated that the phase behavior is resulting from the new thermodynamic equilibrium during sour gas injection as simulated by a swelling test. It showed that increasing the acid content in the injection stream improves the miscibility of the sour/acid gas with reservoir oil due to the higher solubility and swelling, especially in the presence of H_2S. Consequently, the ratio of saturation pressure to original oil bubble point pressure would substantially decrease to a minimum with a pure H_2S stream.

2.5.4 Sour gas injection management

Abou-Sayed et al. developed a comprehensive strategy to effectively manage the production of sour gases, particularly in the area of H_2S management. The key elements needed to comply with regulatory requirements and avert public concern as part of an efficient sour stream management strategy are quoted from the reference and summarized as follows: ‘Maintain the integrity of safety in the operations by minimizing the risks to human health and environmental damage. Maximize the value of the development through informed choices. Convert waste into a resource. Minimize the production of waste.’

Key risks involved when dealing with sour gases have been identified and summarized as follows:

- Integration of acid gas injection (AGI) with other conventional operations.
- Fire or explosion.
- Human behavior and tolerance to H_2S exposure (toxicity).
- Environmental impact caused by H_2S leakage.

- Leakage through surface installations (sulfur plant, rotating equipment).
- Lack of operational experience, Integrity of emergency toolkit, and break out of injection zone (in case of induced fractures).

Having identified the risks, the following options are suggested as ways to deal with the sour gases specifically in offshore fields (Abou-Sayed et al. 2004)$_2$S and CO_2 resulting from the gas sweetening process.H_2S is converted using a sulfur extraction/recovery unit to form solid sulfur blocks which can be stored/disposed above or below the ground while CO_2 is vented to the atmosphere

Disposal of the separated acid gas stream into a deep subsurface geological zone located below a producing reservoir containing unusable formation brine. Sequestration of the acid gas by injecting it into an underground reservoir for storage to be used in the future either as a commercial product (when demand for sulfur/CO_2 increases and is declared economical for production) or as an EOR agent (in the case where a near-by geological reservoir is suitable to under-go miscible gas injection as a tertiary recovery mechanism).

2.5.5 Technical challenges and operational issues in sour gas injection

A sour gas injection program comes with some technical challenges in terms of processing and injecting into the oil reservoir at a pressure as high as 6000psi. Before finalizing the process design, this issue needs to be addressed. Another issue that needs to be addressed when dealing with sour/acid is corrosion. Special materials are required that can handle the corrosive nature of the injection gas for various parts of the facilities. showed that Hydrogen Induced Cracking tested carbon steels with sufficient corrosion allowances should be used for piping, vessels, and equipment.

The gas required several compression stages to maintain the compressed sour gas in a single phase to avoid condensation of H_2S in the sour gas injection facilities. Masahiro et al. show that the total concentration H_2S and CO_2 in the gas fed to the HS-SG compressors should be maintained below 50% in mole. Dehydration is a pre-requisite before high pressure compression to eliminate sulfide stress cracking and CO_2 Corrosion. Literature shows that it is quite difficult to adopt a dehydration unit under high concentration of H_2S over CO_2 due to severe corrosion and sulfur precipitation. However, Masahiro et al. showed that dehydration units were in operation at various sour gas processing plants without any particular problem.

CHAPTER THREE

METHODOLOGY AND MODEL DESCRIPTION

This chapter presents the reservoir model description, detailed methodologies, and procedures used in achieving each objective. The simulation results and discussions are also presented in this chapter for the case and sensitivity study.

3.1 Comparative Study for MMP using Correlations

Multiple-contact miscibility achieved through gas injection is one of the most economical and widely used oil recovery method in the oil industry. The economic success of a gas injection project can be improved by operating at pressures close to MMP. However, this requires accurate experimental measurements of MMP. The currently proposed MMP correlations may be a good substitute for both costly and time consuming experimental measurements.

Unfortunately, most of the MMP correlations are not flexible to represent a variety of solvent/oil combinations. Also, care must be taken when selecting one of them. Reliable MMP correlations must be used for preliminary screening or feasibility studies, but should

not be relied upon. This study provides an evaluation of the existing pure and impure CO_2-stream MMP correlations published in the literature. Three injection scenarios were considered to evaluate the general trend on how MMP changes with a decrease in C_1 composition.

Table 2 : Different Scenarios for MMP studies

Scenario	Component in injection gas	Composition (%)
First Scenario	$CO_2 + C_1$	100
Second Scenario	$CO_2 + H_2S + C_1$	100
Third Scenario	$H_2S + C_1$	100

Table 3: Result of MMP Studies for Scenario one

CO_2 (%)	C_1 (%)	Glaso (Psi)	Yuan et al (psi)
10	90	6799	7948
20	80	6392	7473
30	70	5987	6998
40	60	5580	6524
50	50	5174	6049
60	40	4768	5574
70	30	4362	5100.
80	20	3956	4625
90	10	3550	4150
100	0	3144	3675

First Scenario

In this scenario, the injection gas consists of only CO_2 and C_1. Two different correlations were used in this case Yuan et al. and Glaso correlation. MMP was calculated as C_1

composition decreases and CO_2 increases. Both correlations gave a similar trend; the MMP decreased as C_1 composition decreased as is Figure 12 and 13.

MMP for pure CO_2 was calculated first using the two correlations, for Glaso correlation the MMP is a function of reservoir temperature and intermediate component composition in the reservoir oil (C_2-C_6). While for Yuan et al. the MMP is a function of molecular weight of $C_{7+,}$ molar percentage of intermediates and reservoir temperature. The limitation of this correlation is that the oil used for the regression has molecular weight C_{7+} between the range of 140 to 245. While for the oil in study the M_{C7+} is 250. Also, the molar percentage of the intermediates is between 11.3 to 40.3% and reservoir temperature range from 120°F to 300°F (Yuan et al., 2004).

The fraction of impure and pure MMP is calculated using the Yuan et al. correlation from which the impure MMP for the two correlations is calculated.

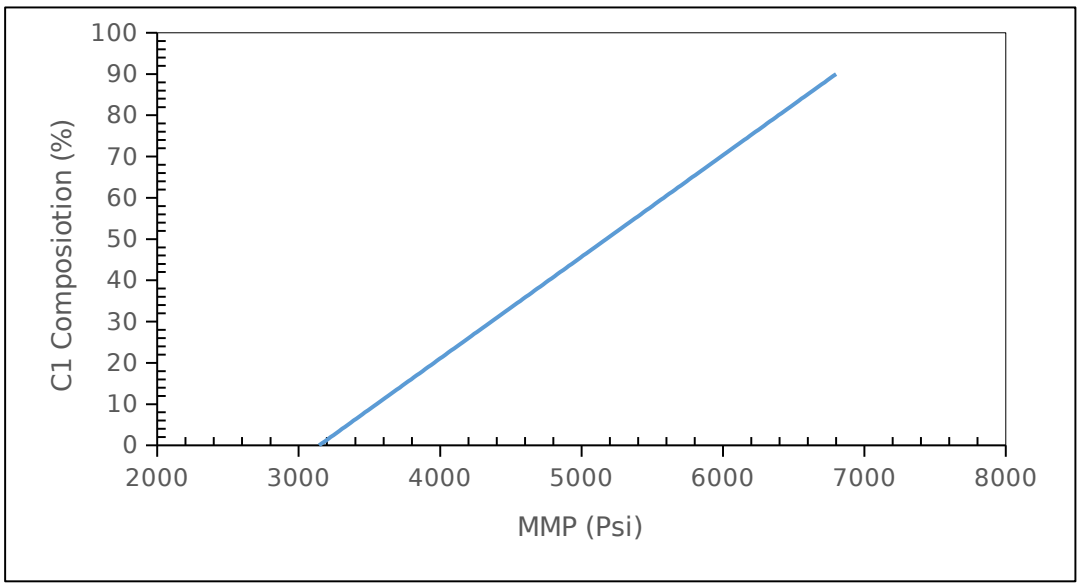

Figure 12: Scenario 1 MMP Change with C1 Composition Using Glaso Correlation

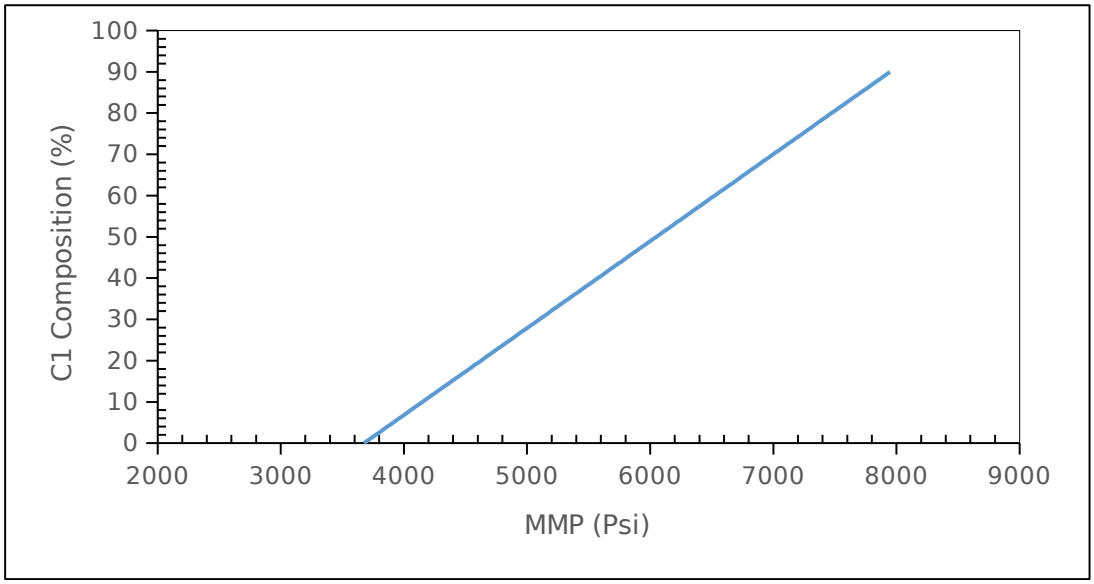

Figure 13: Scenario 1 MMP Change with C_1 Composition Using Yuan et al. Correlation

Second Scenario

In this case, the injection gas consists of three components as listed in Table 7. The injection gas composition changes by decreasing C_1 and increasing H_2S and CO_2. CO_2 and H_2S are increased equally. Two correlations were used for this study, Yuan et al. and Glaso for the estimation of pure CO_2 MMP, for the impure/pure MMP Fraction Sebastian et al. and Yuan et al. are used. While the impure MMP was calculated using Glaso and Yuan et al.

Figure 14 and 15 show the results of the second scenario MMP study using the Glaso and Yuan et al. correlation respectively. Both figures show a linear relationship between C_1 composition and MMP. This scenario shows a similar trend to the first scenario which further confirms the effect of C_1 on MMP. Just as in the first scenario, the Glaso correlation has a more conservative result as compared to Yuan et al. Comparing the result of the two scenarios, the MMP of the second scenario is higher which is due to the presence of H_2S.

Table 4: Result of MMP Studies for Scenario Two

H_2S	CO_2	C_1	Glaso (Psi)	Yuan et al (Psi)

5	5	90	7002	8185
10	10	80	6799	7948
15	15	70	6595	7710
20	20	60	6392	7473
25	25	50	6189	7236
30	30	40	5986	6998
35	35	30	5783	6761
40	40	20	5580	6524
45	45	10	5377	6286
50	50	0	5174	6049

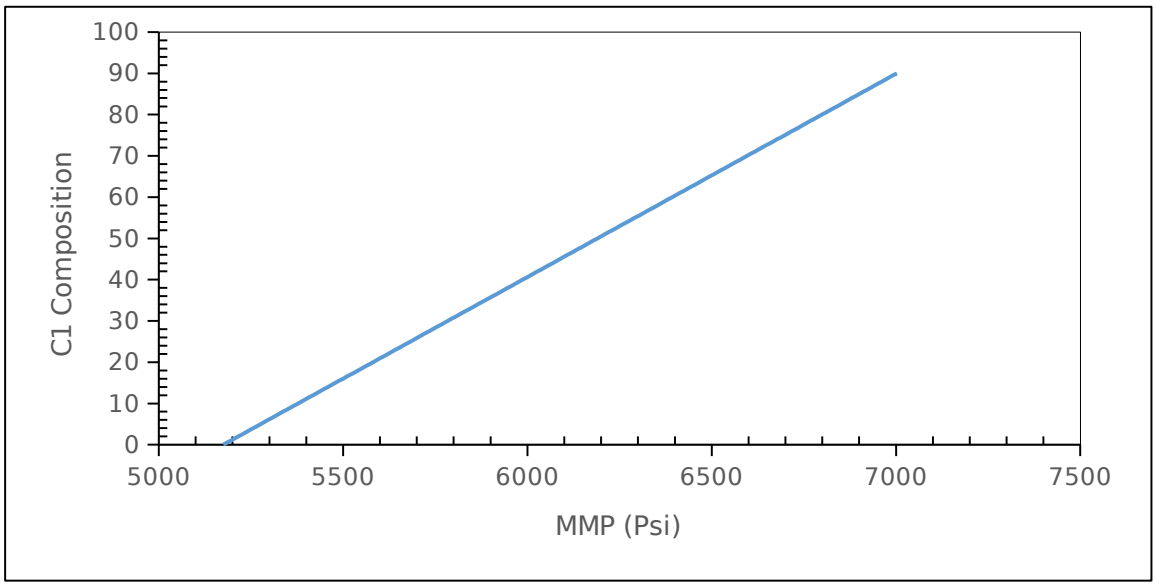

Figure 14: Scenario 2 MMP Change with C_1 composition using Glaso Correlation

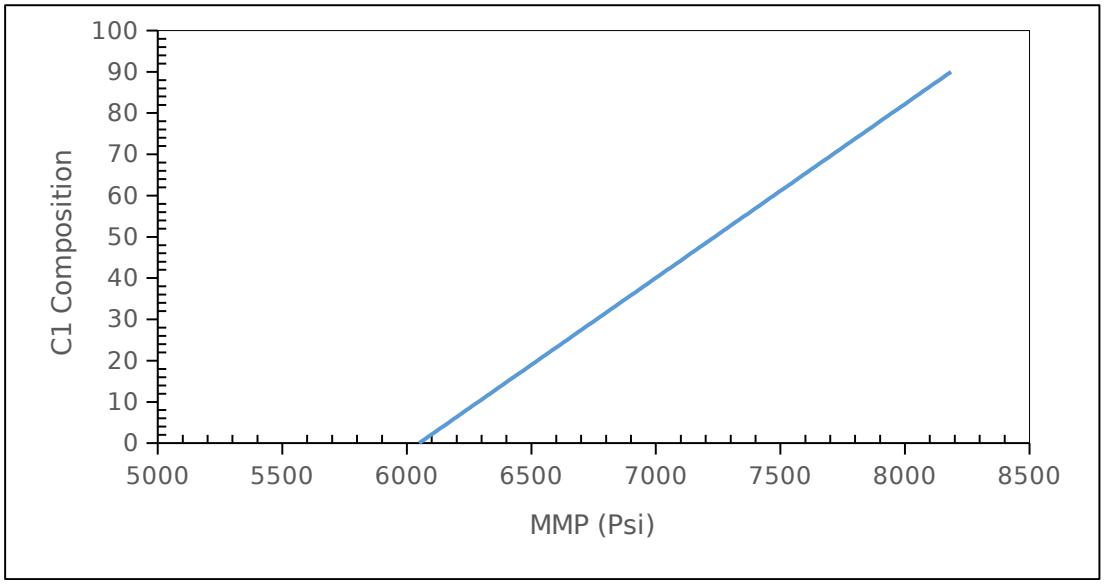

Figure 15; Scenario 2 MMP Change with C_1 composition using Yuan et al. Correlation

Third Scenario

For this part of the study, only H_2S and C_1 are present in the injection gas no CO_2. The goal here is to understand how H_2S affect the MMP. Correlation for estimating hydrocarbon gas MMP and Impure CO_2- stream will be used to calculate the MMP. The Glaso correlation for hydrocarbon gas is the best option because it accounts for the change in C_1 composition in the injected gas which corresponds to the objective of this study. The Yuan et al. correlation is used for the impure CO_2- stream for comparison purpose.

Figure 16 and 17 show the MMP trend for the third scenario using the Glaso and Yuna et al. correlation respectively. It is seen that the Glaso correlation gives a more realistic MMP as compared to Yuan et al. Correlation. This is because Yuan et al. is designed for a CO_2- stream with purities which is not true for this case. However, they both show a parabolic trend, unlike the previous scenarios where a linear trend is seen. This could be associated with the fact that both correlations used are not a perfect match for the case under investigation. The Glaso correlation is designed for gas injection with intermediates component (C_2-C_6) molecular weight of 34 which is not the case here.

Table 5: Result of MMP Studies for Scenario Three

H_2S	C_1	Glaso (Psi)	Yuan et al. (Psi)
10	90	10020	28175
20	80	7029	23835
30	70	5027	19928
40	60	3696	16442
50	50	2823	13366
60	40	2260	10686
70	30	1908	8389
80	20	1700	6464
90	10	1590	4897
100	0	1546	3675

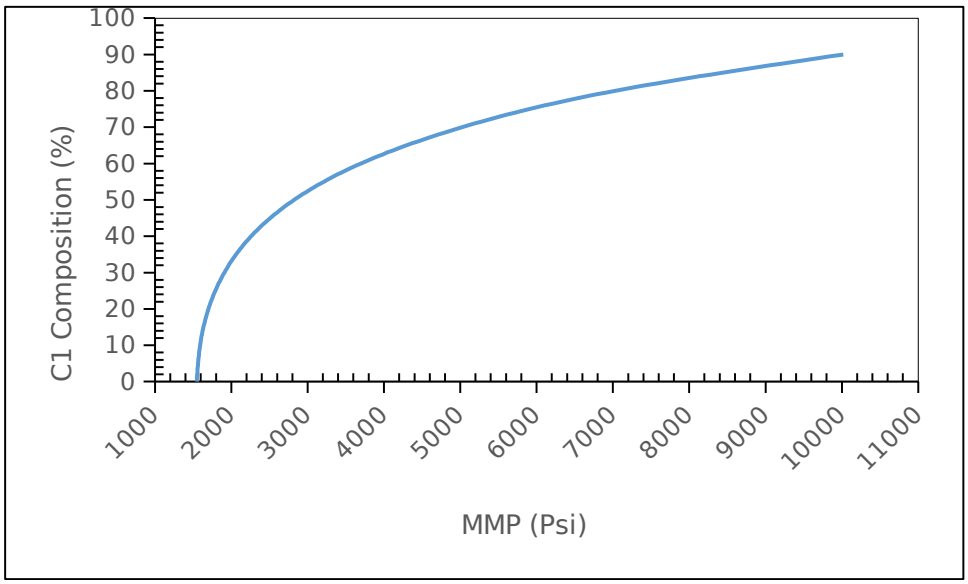

Figure 16: MMP Trend with Changing C1 Composition Using Glaso Correlation

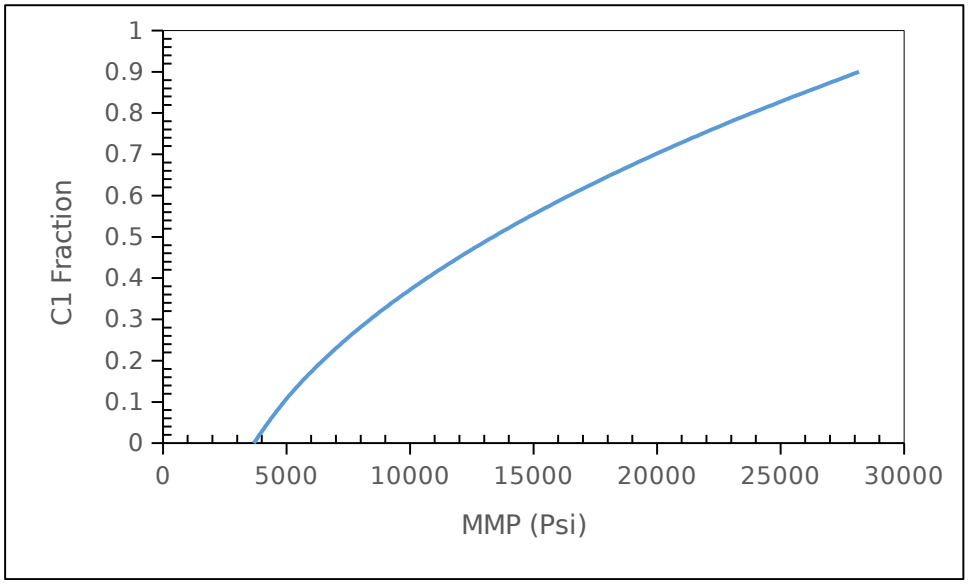

Figure 17: MMP Trend with Changing C1 Composition Using Yuan et al. Correlation

3.2 Base Case Description

The reservoir model in this thesis is based on the reservoir study by (Battistelli et al., 2011).The fluid composition, porosity and initial water saturation are the same as reported. Other parameters such as permeability, grid, reservoir pressure, and temperature were assumed. The base case is modeled as a homogeneous reservoir with both porosity and permeability that is uniform in all direction. The model consists of two wells, one producer and injection. The base case is a homogeneous reservoir model which has a length of 1,320 ft, a width of 1,320 ft and a thickness of 10 ft as shown in Figure 18 and major reservoir parameters are summarized in Table 3. Peng-Robinson EoS is used in fluid characterization, and the component properties are summarized in Table 3. The injection fluid composition is shown in Table 2.

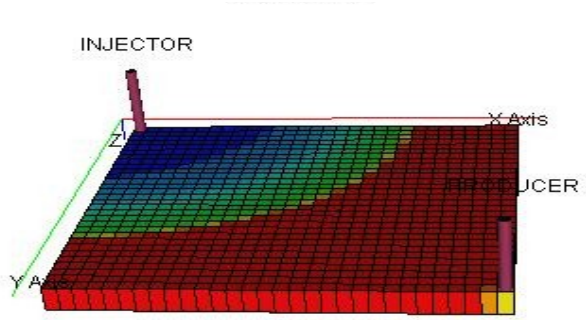

Figure 18: Model Diagram

Table 6: Injection Fluid Composition

Injection Fluid Composition at 100 ºC		
Component	Mole Fraction	Reference
H_2S	0.0735	
CO_2	0.0744	
C1	0.8384	
C2	0.0130	
C3	0.0007	

Table 7: Reservoir Fluid Composition

Reservoir Fluid Composition at 100 ºC (212 ºF)		
Component	Mole Fraction	Reference
H_2S	0.1500	(Battistelli, Ceragioli, and Marcolini 2011)
CO_2	0.0500	

C1	0.4500		
C2	0.0500		
C3	0.0500		
C5	0.0500		
C6+	0.1000		
C9+	0.0939		
H20	0.0061		
Pseudo-Component Properties			
C6+		C9+	
Molecular Weight	**93**	Molecular Weight	**250**
Specific Gravity	**0.29**	Specific Gravity	**0.73**

3.1.4 Reservoir Initialization

The initial field pressure is 5169 psi at a reference depth of 9840 ft, which corresponds to the top of the reservoir. The gas-oil contact is set far above the reservoir so that only the hydrocarbon content is considered for study; the water-oil contact is set at 100 ft below the reference depth.

From Table 4, simple calculation shows that the reservoir has a pore volume of 620,160 rb, with an initial hydrocarbon pore volume of 496,128 rb. The original oil in place, water in place and gas in place are 216,050 STB, 124,128 rb and 570.80 3Mscf respectively. The reservoir has an initial GOR of 2.642 Mscf/STB and FVF of 2.298 rb/STB

Table 8;: Reservoir Model Input parameters

Base model input parameter	
Parameter	Value
Grid	
Cells	Nx=30, Ny=30, Nz=5
Cells dimension	Dx=44ft, Dy=44ft, Dz=2ft
Injection Cells	Nx=1, Ny=1,Nz=1
Production Cells	Nx=30, Ny=30,Nz=5

Porosity	0.2
Permeability	K_v=15 md, K_h=15 md
Reservoir Temperature	212 ^oF
Reservoir Pressure	5169 psi
Wellbore Radius	0.3ft
Oil production rate	Unlimited
Gas Production rate	1000 Mscf/day
Production Well BHP	2000 psi
Gas injection rate	2000 Mscf
Injection well BHP	5200 psi
Simulation Time	800 days

Water Properties	
Compressibility (1/psi)	$3.0x10^{-6}$
Density (lbm/ft3)	63
Rock Compressibility (1/psi)	$4.0x10^{-6}$
Viscosity (Cp)	0.31

Component Properties				
Component	Critical Temp (^oF)	Critical Pressure (psi)	Molecular Weight	Compressibility
CO_2	548.46	1071.33	44.01	0.274077
H_2S	672.48	1296.17	34.076	0.281954
H_2O	473.24	1447.64	18.01	0.275389
C1	343.08	667.781	16.043	0.284729
C2	549.77	708.342	30.07	0.284634
C3	665.64	615.758	44.097	0.276164
C5	838.62	487.169	72.151	0.268808
C6+	957.03	469.530	93	0.272489
C9+	1389.1	207.897	250	0.220257

Table 9: NA phase binary interaction parameters for the components contained in the oil mixture

NA-kij	CO_2	H_2S	H20	C1	C2	C3	C5	C6+	C9+
CO_2									

H_2S	0.096								
H_2O	0	0							
C1	0.1	0.05	0						
C2	0.1	0.05	0	0					
C3	0.1	0.05	0	0	0				
C5	0.1	0.05	0	0	0	0			
C6+	0.1	0.05	0	0.0326	0.01	0.01	0		
C9+	0.1	0.05	0	0.0512	0.01	0.01	0	0	0

Table 10: Oil, Water and Gas Saturation Functions

SW	KRW	PCOW	SO	KROW	KROG	SG	KRG	PCOG
0.2	0	0	0	0	0	0	0	0
0.24	0.003	0	0.3	0	0	0.05	0	0
0.28	0.01	0	0.33	0.005	0.005	0.1	0.004	0
0.32	0.023	0	0.36	0.018	0.018	0.15	0.015	0
0.36	0.04	0	0.39	0.038	0.038	0.2	0.033	0
0.4	0.063	0	0.42	0.064	0.064	0.25	0.059	0
0.44	0.09	0	0.45	0.096	0.096	0.3	0.093	0
0.48	0.123	0	0.48	0.133	0.133	0.35	0.133	0
0.52	0.16	0	0.51	0.175	0.175	0.4	0.181	0
0.56	0.203	0	0.54	0.223	0.223	0.45	0.237	0
0.6	0.25	0	0.57	0.275	0.275	0.5	0.3	0
0.64	0.303	0	0.6	0.333	0.333	0.55	0.37	0
0.68	0.36	0	0.63	0.395	0.395	0.6	0.448	0
0.72	0.423	0	0.66	0.462	0.462	0.65	0.533	0
0.76	0.49	0	0.69	0.533	0.533	0.7	0.626	0
0.8	0.563	0	0.72	0.609	0.609	0.75	0.726	0
0.84	0.64	0	0.75	0.69	0.69	0.8	0.834	0
0.88	0.723	0	0.78	0.775				0.775
0.92	0.81	0	0.8	0.834				0.834
0.96	0.903							0
1	1							0

CHAPTER FOUR

RESULTS AND DISCUSSIONS

Compositional Variation of Acid gas in the Injection Gas

This study aimed to determine how acid gas concentration in the injection gas affects oil recovery. It also helps to understand how acid gas helps to improve recovery in a gas injection process. A 15-mole percent acid gas is used for the base case model with an equal composition for H_2S and CO_2 (i.e., 7.5% of H_2S and 7.5% CO_2). C_1 makes up 80% of the injection gas, 0.0061% water while C_2-C_5 makes up the remaining percentage as shown in Table 2.

Figure 19 shows the effect of acid gas on oil recovery efficiency. The result shows that the increase of acid gas concentration gives the increases of oil recovery. An overall recovery of 86.81 and 78% was achieved for 40.30 and 20% acids gas composition respectively.

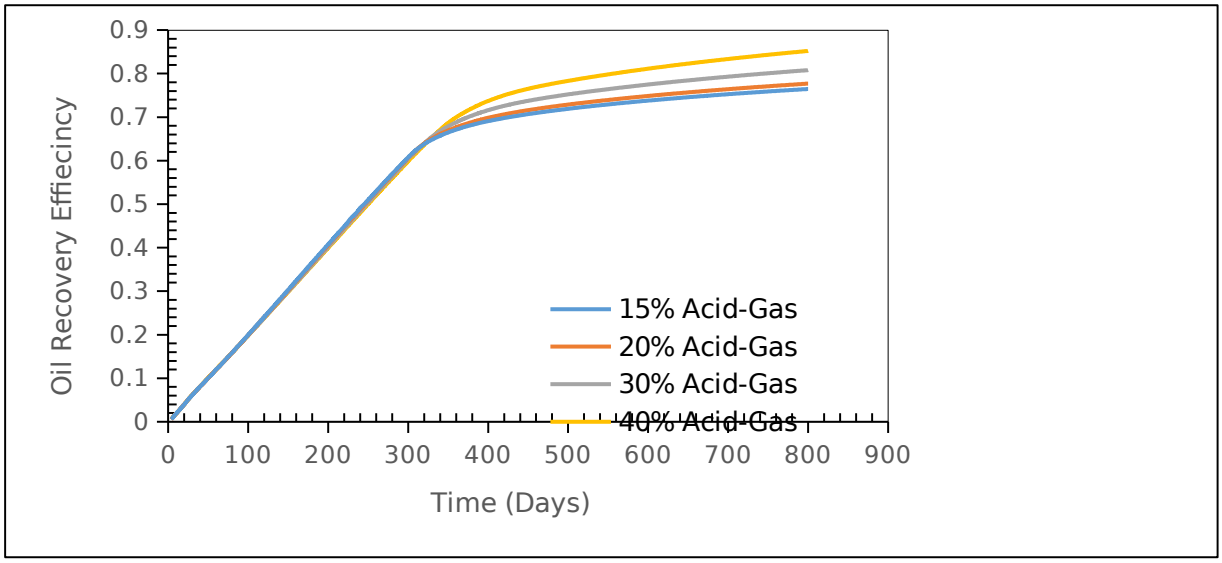

Figure 19: Comparison: The effect of acid gas composition on oil recovery efficiency

Figure 20 shows how acid gas composition affects oil production rate. The result clearly shows that as the composition of acid gas increases the gas breakthrough time also increases. This is because as the acid gas increases the viscosity of the injection gas also increases.

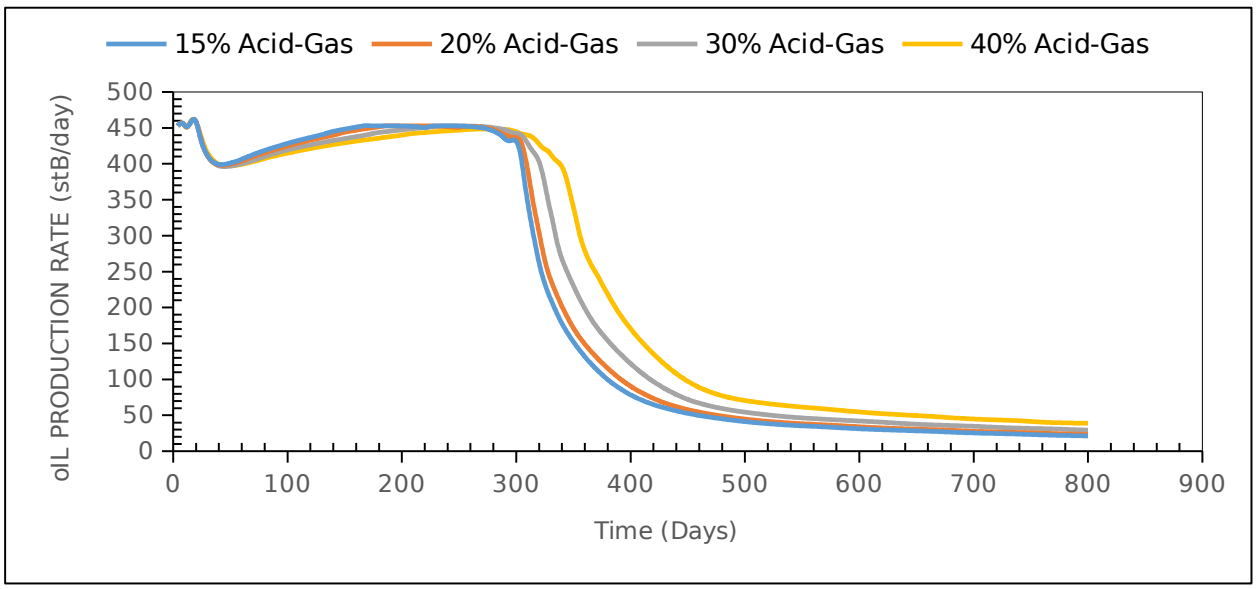

Figure 20: Comparison: The effect of Acid Gas Composition on Oil Production Rate

Figure 21 shows the gas production rate. The first down dip is when the reservoir is producing under natural depletion before injection starts. Compare the base case, as the

pressure support starts at around day 100 there is a plateau gas production while for 40% acid gas, the gas production didn't stabilize until after the gas breakthrough.

Figure 22 shows the change in gas viscosity with increased acid gas concentration. This gives a clearer picture on the production profile of both gas and oil. This figure shows that the gas viscosity increases as acid gas concentration is increased. The increase in gas viscosity is the consequence of miscible development resulting in a reduction of oil viscosity

This reduction is the result of oil swelling or expansion of the under-saturated fluid by the addition of dissolved gas at higher pressures, which lightens the oil and consequently decreases the oil viscosity. This is why for 40% of the acid gas profile didn't reach a plateau production until after gas breakthrough. As a result, more gas dissolving in oil means less gas is coming out of solution.

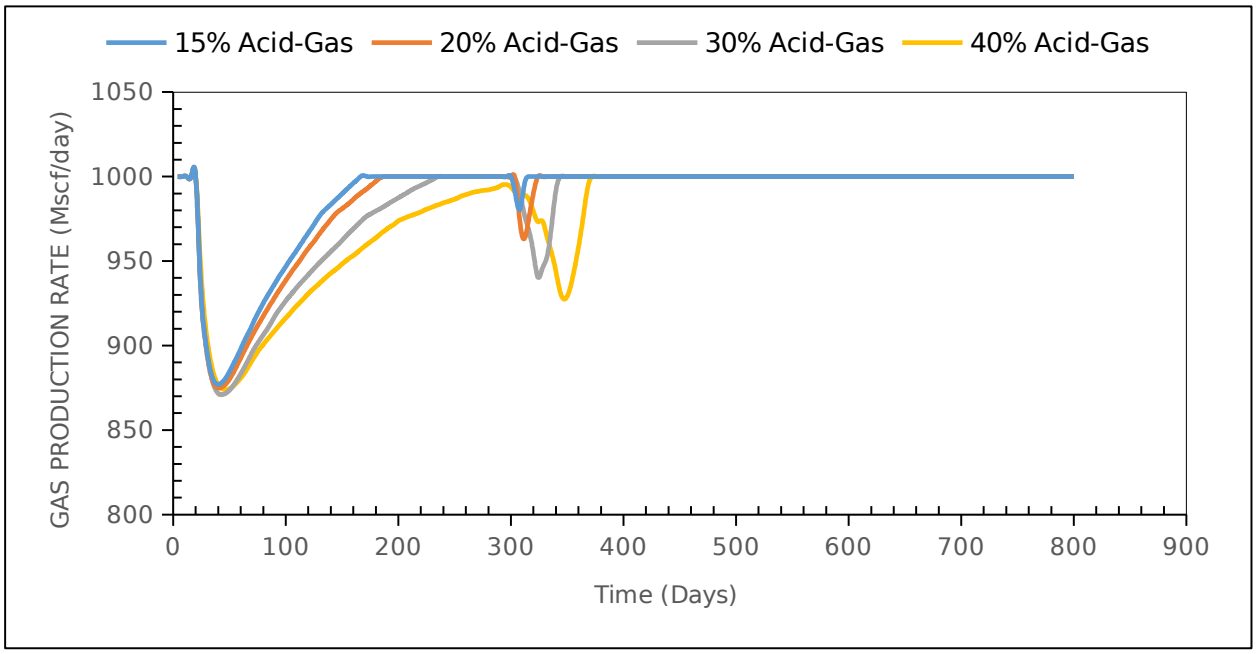

Figure 21 Comparison: The effect of Acid Gas Composition on Gas Production Rate

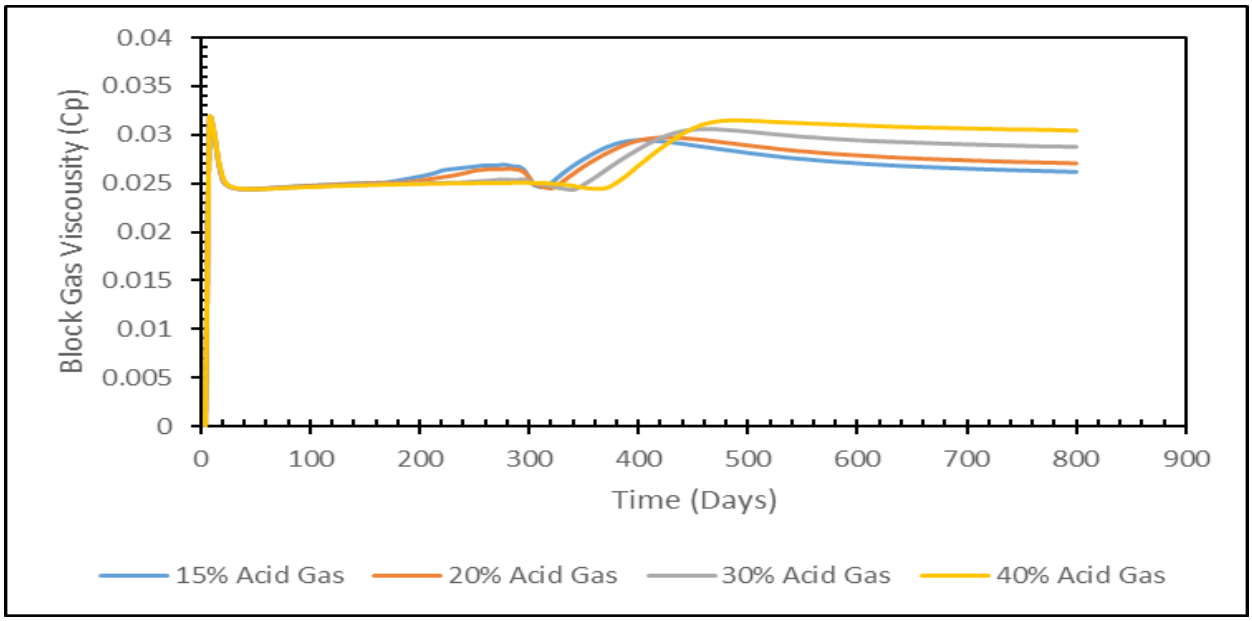

Figure 22: Effect of Acid Gas Composition on Gas Viscosity in the Production Block

Effect of gas injection rate

The aim of this study was to understand how gas injection rate affects various parameters such oil recovery, oil production rate and how the volume of gas injected increases oil recovery. For this study, three rates were used to compare with the base case model. The injection was changed from 500 to 3000Mscf to compare with the base case of 2000Mscf.

Figure 23 shows how the gas injection rate affects oil production rate. It was observed that there was an early gas breakthrough for rate 2000 and 3000Mscf. This could be due to the increase in driven force as the injection rate increases. There was no noticeable change when the injection rate increased above 2000Mscf. This is because the injection-well is constrained using two parameters (injection rate and pressure).

Figure 24 shows the injection rate builds up over time. From the result, it is seen that the rate is gradually building up to the constrained rate and maintained throughout the simulation time for 500Mscf and 1000Mscf. While for 2000 and 3000Mscf the rate gradually builds up until the pressure support kicks in. But the rate does exceed 1500Mscf which is maintained

until the gas breakthrough after which rate starts declining until it reaches 1000Mscf. This further shows that the current injection pressure doesn't support any rate above 1500Mscf. The rate of decline after breakthrough is due to the decrease in pressure support.

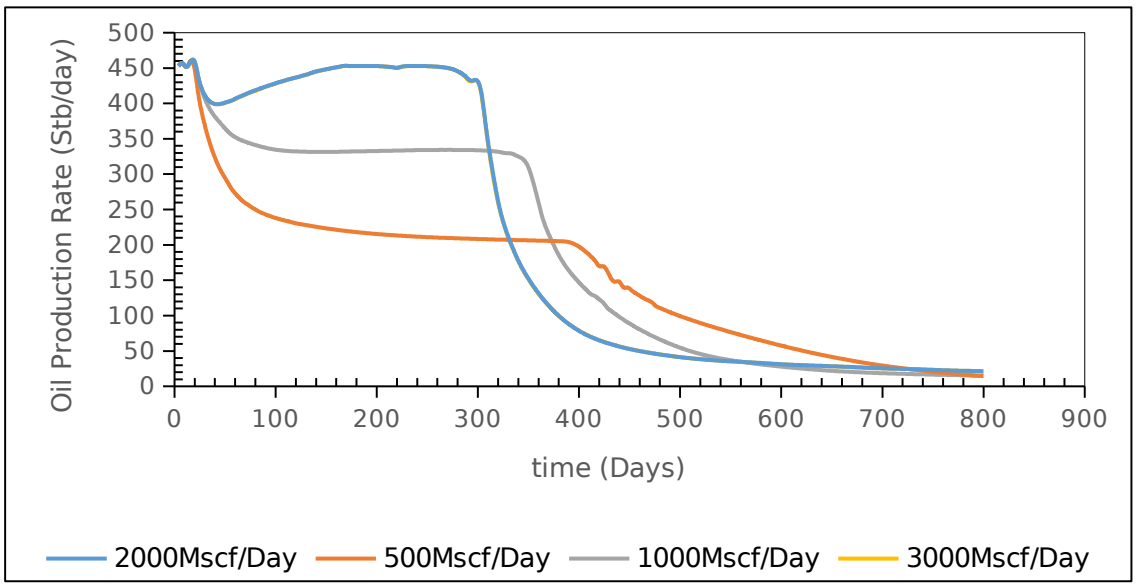

Figure 23: Comparison: Effect gas injection rate on oil Production Rate

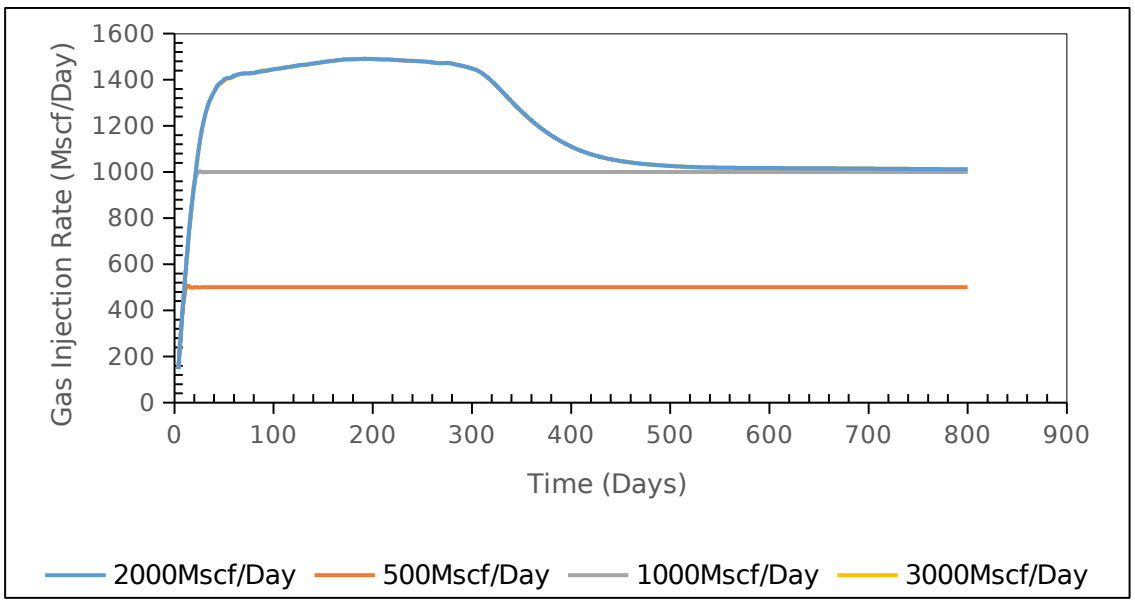

Figure 24: Gas injection rate vs. time

Figure 25 is used to investigate how the volume of gas injected affects oil recovery efficiency. The result clearly shows the volume of gas injected is directly proportional to oil recovery efficiency. The result is consistent with the findings of (Comberiati and

Zammerilli,2000) which also showed an increment in oil production with increasing flood volume.

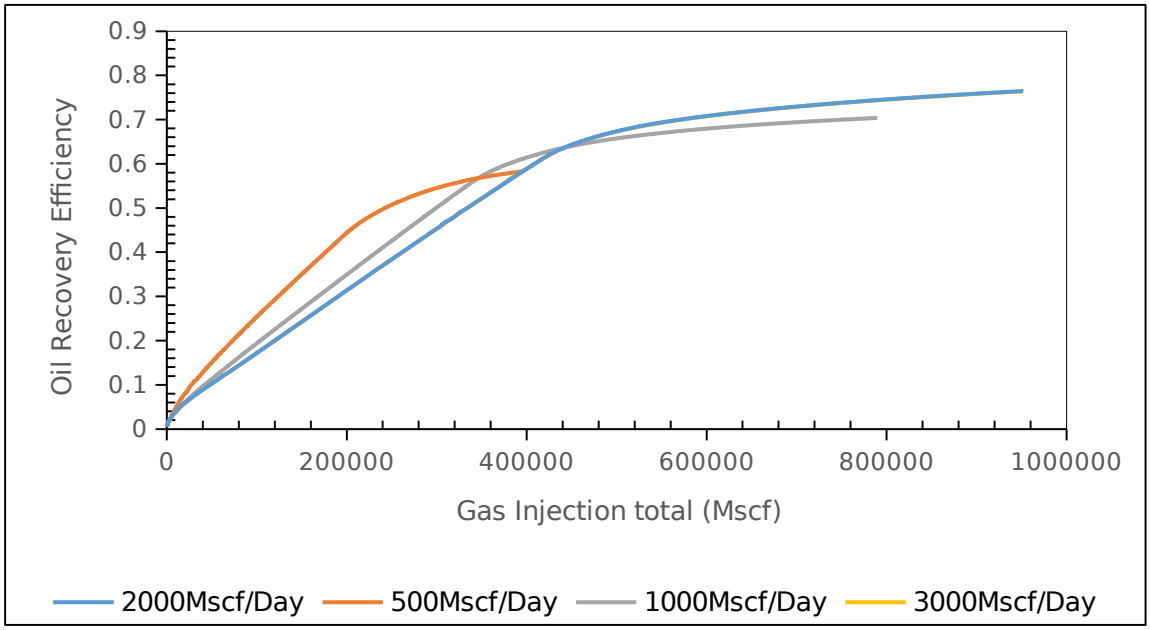

Figure 25: Cumulative gas Injected Vs Oil Recovery efficiency

3.2.3 Injection Pressure Effect

In this part of the study, the effect of injection pressure on the oil recovery from the model was investigated. Injection and production wells are completed in the first and fifth layer, respectively. For this investigation, two different pressures were used representing low case and high case to compare with the base case model.

For low case, an injection pressure of 2500psia was used. This pressure was used to simulate immiscible gas injection. While for the high case, an injection pressure of 7500psia was used which simulates first contact miscible injection. Based on the MMP study done, estimated MMP based on the equation of state analytical method using the Eclipse PVTi is approximately 6200 psia for first contact miscibility and 5000 psia for multi-contact

miscibility. Simulation runs were conducted at pressures below, equal to and greater than this pressure as stated above.

Since in vaporizing drive mechanisms, the pressure at miscible front should be greater than the predicted miscible pressure, injection of gas at 5,200 psi will raise the average reservoir pressure from initial pressure to the miscibility pressure of 5000 psi. Therefore, the injection pressure of 5,200 psi seems to be the best candidate for the base case model. It is clearly seen in Figure 26 that there is an incremental oil recovery as a result of an increase in injection pressure.

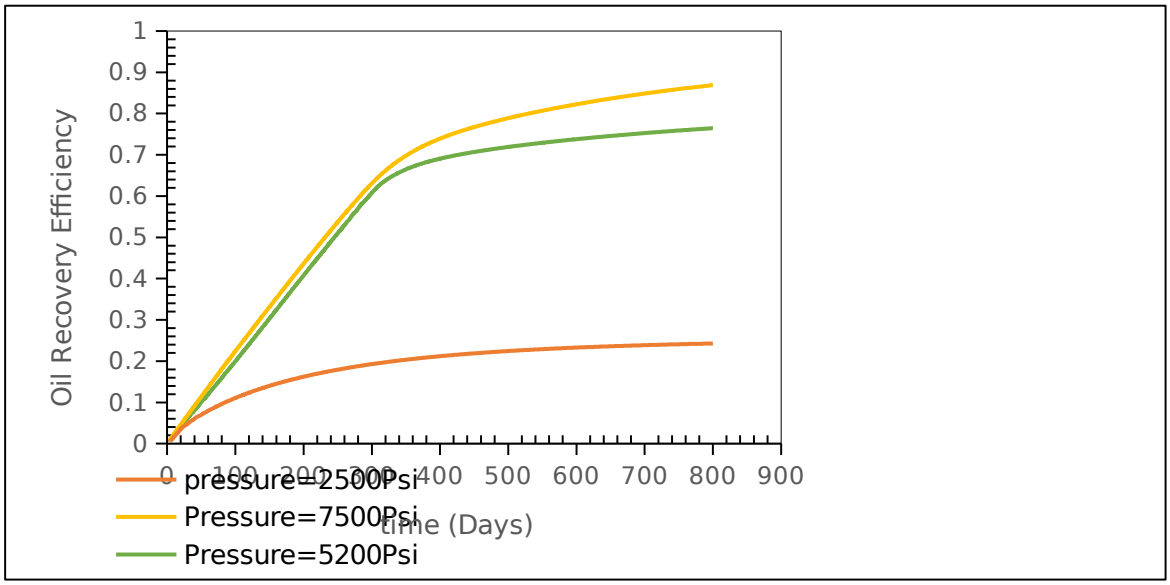

Figure 26: Effect of gas injection pressure on oil recovery efficiency

Figure 27 shows the oil production rate for different injection pressure. According to the figure, for the high case the pressure support was almost immediate while for the base case the pressure support didn't kick in until after 52 days of continuous gas injection. High case shows an early breakthrough time, but the difference as compared with the base case is marginal which further supports the argument that the economy may not support the incremental recovery from the high case.

Figure 28 shows the gas injection rate at different injection pressure. The figure shows how injection pressure affects the gas injection rate. For high case, a rate of 2000Mscf was maintained until after the gas breakthrough. After which there was a steady decline in the rate till it reached 1000Mscf. This effect was seen during the injection rate study which further proves that the injection rate is directly proportional to injection pressure. This is due to the fact that high injection pressure means the driven force is high which translates to high gas velocity. It shows that for this study the 1000Mscf rate is the optimal injection rate though no economic analysis has been done.

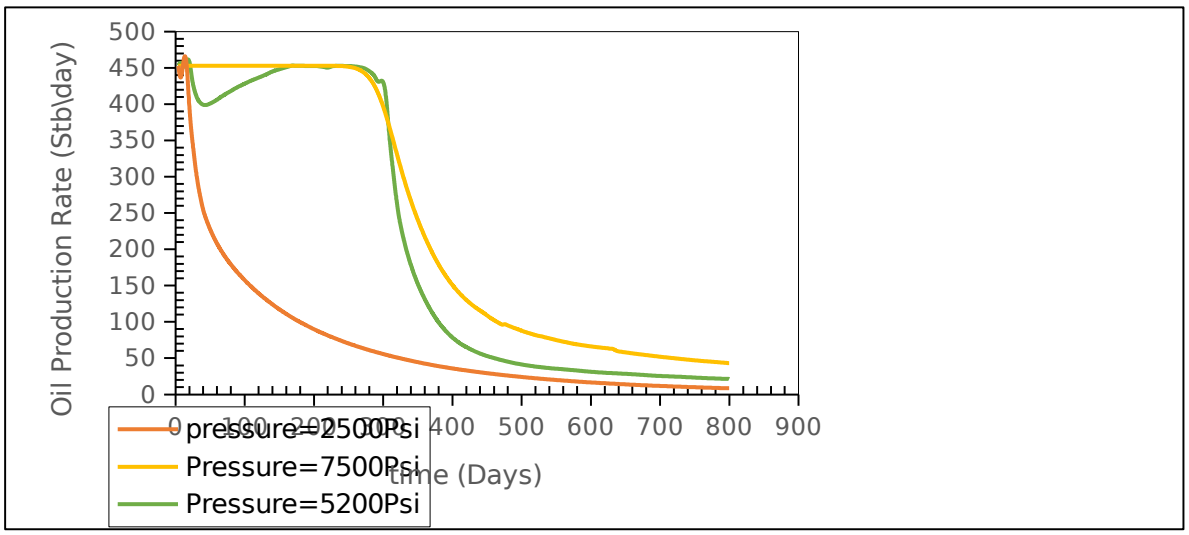

Figure 27: Effect of gas injection Pressure on Oil Production rate

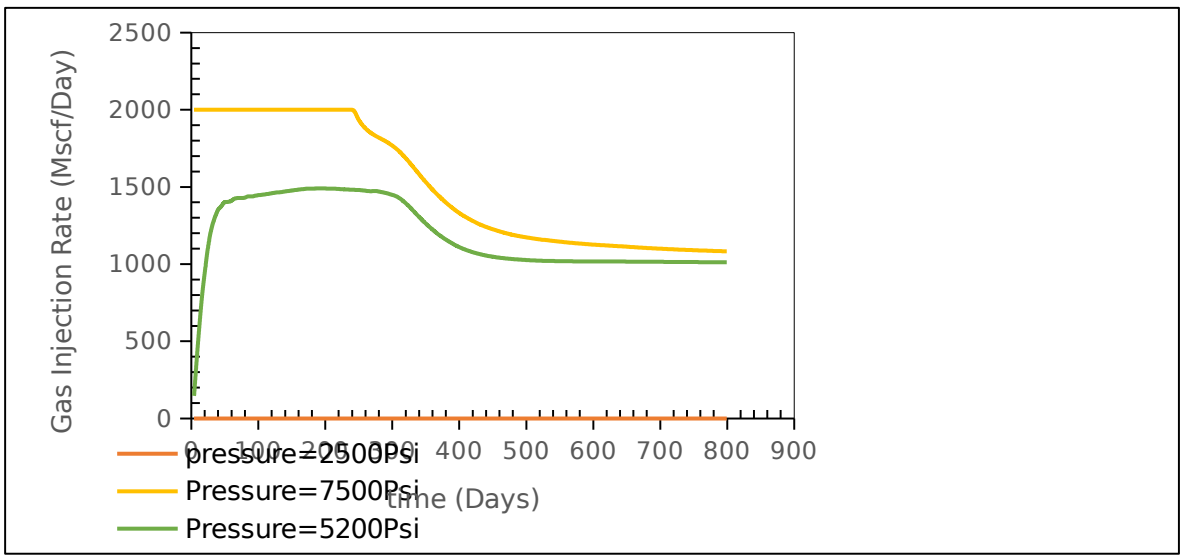

Figure 28: Effect of gas injection pressure on injection rate

CHAPTER FIVE

Conclusion and Recommendation

5.1 Conclusion

In conclusion sour gas injection for enhancing oil recovery has supreme performance as compared to other gases used for miscible gas flooding EOR. Acid gas can lower the MMP of the process significantly resulting in more oil recovery and low operational cost for the process. The success of miscible gas injection EOR can be attributed to the variation in fluid viscosities toward lower mobility ratios during injection. Injection gas lowers the oil viscosity substantially. This reduction is as the result of oil swelling or expansion of the under-saturated fluid by the addition of dissolved gas at higher pressures, which lightens the oil and consequently decreases the oil viscosity.

5.2 Recommendations

When designing a sour gas injection process, acid gas composition should be the key design parameter because it directly affects the MMP of the process which, if optimized can make the economics of the process favorable. For an effective injection process, hydrocarbon composition more specifically, C_1 should be kept as low as possible as it has a reverse effect on acid gas in the injection gas.

For future research, some of the following recommendations are made in order to improve on this work.

1. This study was conducted on a homogenous model for future work the effect of reservoir heterogeneity should be investigated.
2. The study should be conducted on actual field data, based on the result of this study sour gas injection for EOR is technically feasible. Economics analysis should be

conducted to determine whether this project will add value, in essence, to see if the economics is favorable.

3. Another interesting area to look into is hydration formation and asphaltene deposition during sour gas injection to develop a strategy on how to handle this problem.
4. Assessing the effect of injecting a higher concentration of acid gas and the thermodynamic equilibrium that may occur from the processes it impacts on formation porosity, permeability and well injectivity.

REFERENCES

1. Abou-Sayed, Ahmed S, Zaki, Karim, Summers, and. Chris. 2004. "Management of Sour Gas by Underground Injection - Assessment, Challenges and Recommendations." SPE: Society of Petroleum Engineers. doi: 10.2118/86605-MS.
2. Ahmed, T., and P. McKinney. 2005. *Advanced Reservoir Engineering*. Burlington, MA:: Elsevier.
3. Al-Hadhrami, Abdullah Khalifa., Darrell Wayne. Davis, Geurt. Deinum, and Harry. Soek. 2007. "The Design of the First Miscible Sour Gasflood Project in Oman." IPTC: International Petroleum Technology Conference. doi: 10.2523/IPTC-11396-MS.
4. Battistelli, Alfredo, Paola Ceragioli, and Marica Marcolini. 2011. "Injection of Acid Gas Mixtures in Sour Oil Reservoirs: Analysis of near-Wellbore Processes with Coupled Modelling of Well and Reservoir Flow." *Transport in Porous Media* 90 (1): 233-251. doi: 10.1007/s11242-010-9685-6.
5. Benham, A.L., W.E. Dowden, W. Kunzman, and J. 1960. "Miscible Fluid Displacement-Prediction of Fluid Miscibility."
6. *Petroleum Transactions, AIME* 219: 8.
7. Bennion, D. B., F. B. Thomas, D. W. Bennion, and R. F. Bietz. 1999. "Formation Screening to Minimize Permeability Impairment Associated with Acid Gas or Sour Gas Injection/Disposal." doi: 10.2118/99-13-56.
8. Bierlein, James. A., and Webster. B. Kay. 1953. "Phase-Equilibrium Properties of System Carbon Dioxide-Hydrogen Sulfide." *Industrial and Engineering Chemistry* 45 (3): 6. doi: DOI: 10.1021/ie50519a043.

9. Ceragioli, P, and G. Gianelli. 2008. "Alteration of Thermodynamic Equilibria and Fluids-Rock Interactions During Acid Gas Injection into a Carbonate Sour Oil Reservoir." SPE: Society of Petroleum Engineers. doi: 10.2118/113920-MS.
10. Chen, Z., X. Liao, X. Zhao, C. Chen, L. Zhu, F. Zhang, L. Mu, and X. Zhou. 2016. "Optimization of Injection and Production Parameters for Sour Gas Storages: A Case Study." OTC: Offshore Technology Conference. doi: 10.4043/26686-MS.
11. Christiansen, Richard L., and Haines. Kim. 1987. "Rapid Measurement of Minimum Miscibility Pressure with the Rising-Bubble Apparatus." doi: 10.2118/13114-PA.
12. Chugh, Shelin, Jens Behrend, Robert McKishnie, and Aaron. 2006. "Development of the Strasshof Tief Sour Gas Field Including Acid Gas Injection into Adjacent Producing Sour Gas Reservoirs." SPE: Society of Petroleum Engineers. doi: 10.2118/100328-MS.
13. Cotter, W.H. 1962. "Twenty-Three Years of Gas Injection into a Highly Undersaturated Crude Reservoir." *J Pet Technol* 14 (4): 4. doi: http://dx.doi.org/10.2118/82-PA.
14. Danesh, Ali. 2007. *Pvt and Phase Behaviour of Petroleum Reservoir Fluids*. Amsterdam: Elsevier.
15. E. Ghoodjani, and . S.H. Bolouri. 2011. "Experimental Study of Co2-Eor and N2-Eor with Focus on Relative Permeability Effect." *Journal of Petroleum & Environmental Biotechnology* 53 (2): 9.
16. Eakin, B.E., and F.J. Mitch. 1988. "Measurement and Correlation of Miscibility Pressure of Reservoir Oil " In *SPE Annual Technical Conference and Exhibition, Houston*. SPE.

17. Elsharkawy, A. M., F. H. Poettmann, R. Christiansen, and L. 1992. "Measuring Minimum Miscibility Pressure: Slim-Tube or Rising-Bubble Method?". SPE: Society of Petroleum Engineers. doi: 10.2118/24114-MS.
18. Firoozabadi, Abbas, and Aziz Khalid. 1986. "Analysis and Correlation of Nitrogen and Lean-Gas Miscibility Pressure(Includes Associated Paper 16463)." doi: 10.2118/13669-PA.
19. Glaso, O. 1985. "Generalized Minimum Miscibility Pressure Correlation (Includes Associated Papers 15845 and 16287)." doi: 10.2118/12893-PA.
20. Green, Don W., and G Paul. Willhite. 1998. *Enhance Oil Recovery, Spe*. USA: SPE.
21. Haynes, Byron, Naveen Chander Kaura, and Andrew Faulkner. 2008. "Life Cycle of a Depletion Drive and Sour Gas Injection Development: Birba A4c Reservoir, South Oman." IPTC: International Petroleum Technology Conference. doi: 10.2523/IPTC-12175-MS.
22. Hinderaker, Leif, Rolf H. Utseth, Odd Steve Hustad, Idar Akervoll, Mariann Dalland, Bjorn Arne Kvanvik, Tor Austad, and John Eirik Paulsen. 1996. "Ruth - a Comprehensive Norwegian R & D Program on Ior." SPE: Society of Petroleum Engineers. doi: 10.2118/36844-MS.
23. Holm, L. . 1986. "Miscibility and Miscible Displacement. ." *Journal of Petroleum Technology* 38: 1.
24. Holm, L. W., and V. A. Josendal. 1974. "Mechanisms of Oil Displacement by Carbon Dioxide." doi: 10.2118/4736-PA.
25. Hudgins, David A., Feliciano M. Llave, Chung, and T. H. Frank. 1990. "Nitrogen Miscible Displacement of Light Crude Oil: A Laboratory Study." doi: 10.2118/17372-PA.

26. Iman, Farzad., and Amani. Mahmood. 2012. "An Analysis of Reservoir Production Strategies in Miscible and Immiscible Gas Injection Projects." *Advances in Petroleum Exploration and Development* 3 (1): 15. doi: DOI:10.3968/j.aped.1925543820120301.160.
27. Johns, R. T., P. Sah, Solano, and R. 2002. "Effect of Dispersion on Local Displacement Efficiency for Multicomponent Enriched-Gas Floods above the Minimum Miscibility Enrichment." doi: 10.2118/75806-PA.
28. Karim, Khan. MSc, SPEC. 2017. Review of Enhanced Oil Recovery by Non-Hydrocarbon Gas Injection in Carbonate Reservoirs. (35),
29. Khan, Chawarwan, Robert Amin, and Gary Madden. 2013. "Effects of Co2 and Acid Gas Injection on Enhanced Gas Recovery and Storage." *Journal of Petroleum Exploration and Production Technology* 3 (1): 55-60. doi: 10.1007/s13202-012-0044-8.
30. Kovarik, F.S. 1985. "A Minimum Miscibility Pressure Study Using Impure Co2 and West Texas Oil Systems:Data Base, Correlations, and Compositional Simulation." In *SPE Production Technology Symposium, Lubock, Texas*. SPE.
31. Lake, L. W. 1989. *Enhanced Oil Recovery*. Englewood Cliffs, New Jersey: Prentice Hall,.
32. Linderman, John Thomas, Faisal Salah Al-Jenaibi, Saleem G. Ghori, Kevin Putney, John Lawrence, Michel Gallat, and Kurt Hohensee. 2008. "Feasibility Study of Substituting Nitrogen for Hydrocarbon in a Gas Recycle Condensate Reservoir." SPE: Society of Petroleum Engineers. doi: 10.2118/117952-MS.
33. Lyons, W., and Plisga. 2005. *Standard Handbook of Petroleum & Natural Gas Engineering*. Second edition ed. Burlington MA: Elsevier Inc.

34. Manrique, E.J., V.E. Muci, Gurfinkel, and M.E. 2007. "Eor Field Experiences in Carbonate Reservoirs in the United States.". *SPE Reserv. Eval. Eng* 10: 667-686.
35. Masahiro, Miwa, Yuji Shiozawa, Saito Yoshiharu, and Ihab Othman Tarmoom. 2002
36. "Sour Gas Injection Project." SPE: Society of Petroleum Engineers. doi: 10.2118/78547-MS.
37. Menzie, D. E., and R. F. Nielsen. 1963. "A Study of the Vaporization of Crude Oil by Carbon Dioxide Repressuring." doi: 10.2118/568-PA.
38. Metcalfe, R. S., D. D. Fussell, J. Shelton, and L. 1973. "A Multicell Equilibrium Separation Model for the Study of Multiple Contact Miscibility in Rich-Gas Drives." doi: 10.2118/3995-PA.
39. Monroe, Wesley W., Matthew K. Silva, L. L. Larson, and Franklin M. Orr, Jr. 1990. "Composition Paths in Four-Component Systems: Effect of Dissolved Methane on 1d Co2 Flood Performance." doi: 10.2118/16712-PA.
40. Moritis, G. 1995. "Impact of Production and Development Rd and D Ranked." *Oil and Gas Journal*: Medium: X; Size: pp. 37-39.
41. ———. 2008. "Worldwide Eor Survey." *Oil and Gas Journal* 106: 41–42, 44–59.
42. Ogienagbon, Adijat., Oluwaseun Ayodele. Taiwo, Abbas. Mamudu, and Olalekan. Olafuyi. 2016. "Experimental Investigation of the Feasibility of Polymer Flooding in a Shallow Niger Delta Oil Reservoir." SPE: Society of Petroleum Engineers. doi: 10.2118/184297-MS.
43. Orr, F. M., Jr., and M. K. Silva. 1987. "Effect of Oil Composition on Minimum Miscibility Pressure-Part 2: Correlation." doi: 10.2118/14150-PA.
44. Orr, F. M., Jr., M. K. Silva, C. L. Lien, and M. T. Pelletier. 1982. "Laboratory Experiments to Evaluate Field Prospects for Co2 Flooding." doi: 10.2118/9534-PA.

45. Rahmatabadi, K. A. . 2011. "Advances in Calculation of Minimum Miscibility Pressure." The University of Texas at Austin.
46. Romero-Zeron, Laura. 2012. "Advances in Enhanced Oil Recovery Processes." In *Introduction to Enhanced Oil Recovery (Eor) Processes and Bioremediation of Oil-Contaminated Sites*, ed. Laura Romero-Zerón. InTech.
47. Satter, A. , G. Iqbal, and J. Buchwalter. 2008. *Practical Enhanced Reservoir Engineering*. Tulsa, Oklahoma: PennWell.
48. Siddiqui, Muhammad Ibad., Shahzaib. Baber, Waleed Anwar. Saleem, Mohammad Osama. Jafri, and Qaiser. Hafeez. 2013. "Industry Practices of Sour Gas Management by Reinjection: Benefits, Methodologies, Economic Evaluation and Case Studies." SPE: Society of Petroleum Engineers. doi: 10.2118/169645-MS.
49. Stalkup, F. I. 1987. "Displacement Behavior of the Condensing/Vaporizing Gas Drive Process." SPE: Society of Petroleum Engineers. doi: 10.2118/16715-MS.
50. Van Vark, W., S. K. Masalmeh, J. van Dorp, M. Abu Al Nasr, and S. Al-Khanbashi. 2004. "Simulation Study of Miscible Gas Injection for Enhanced Oil Recovery in Low Permeable Carbonate Reservoirs in Abu Dhabi." SPE: Society of Petroleum Engineers. doi: 10.2118/88717-MS.
51. Yellig, W. F., and R. S. Metcalfe. 1980. "Determination and Prediction of Co2 Minimum Miscibility Pressures (Includes Associated Paper 8876)." doi: 10.2118/7477-PA.
52. Zhou, D., and F. M. Orr, Jr. 1998. "An Analysis of Rising Bubble Experiments to Determine Minimum Miscibility Pressures." doi: 10.2118/30786-PA.
53. Zick, A. A. 1986. "A Combined Condensing/Vaporizing Mechanism in the Displacement of Oil by Enriched Gases." SPE: Society of Petroleum Engineers. doi: 10.2118/15493-MS.

NOMENCLATURE

API=American petroleum institute

EOR=efficient oil recovery

FVF = Formation Volume Factor

FCMP=first contact miscibility pressure

GOR= gas/oil ratio, Mscf/STB

HCPV= Hydrocarbon Pore volume

IFT=interfacial tension

IMPES=implicit-pressure explicit-saturation

LPG=Liquified petroleum gas

M_{C7+}=molecular weight of heptane-plus fraction, lb/lbmol

MMP= minimum miscibility pressure, psi

MCM = Multi Contact Miscibility

Mscf=thousand standard cubic feet

M_{c5+} =molecular weight of pentane plus

n=number of components in the solvent

OOIP= originally oil in place, STB

Ppc=pseudo critical pressure of the reservoir fluid, psi

Ppr=pseudo reduced pressure of the reservoir fluid

PR-EOS=Peng-Robinson equation of sate

RBA=rising bubble apparatus

STO=standard tank oil

STB= standard tank barrel

X= molecular weight of C2through C6 components in injection gas, lbm/mol

X_{int}=mole percent of intermediate components (C2through C5)

X_{vol} = mole fraction of volatile components in the oil (C1 and N2)

y= corrected molecular weight of C_{7+}in the stock-tank oil, lbm/mole

y_{C2+}= mole fraction of plus ethane

yi = mole fraction of component i in the solvent

z= mole percent methane in injection gas

APPENDIX

Data file for compositional model

RUNSPEC
==========

FIELD

OIL

WATER

GAS

AIM

COMPS

9 /

EOS

--Peng-Robinson equation of state to be used

PR /

TABDIMS

1 1 40 40 /

DIMENS

30 30 5 /

EQLDIMS

1 20 /

WELLDIMS

2 2 /

START

1 Nov 2017 /

GRID

==========

INIT

--Basic grid block sizes DX 33FT, DY 66FT FOR EACH BLOCK...

-- DZ 5FT FOR EACH LAYER

EQUALS

--VALUE X X Y Y Z Z

DX 44   1 30 1 30 1 5 /

DY 44   1 30 1 30 1 5 /

DZ 2   1 30 1 30 1 5 /

/

-- Porosity and permeability

PORO

4500*0.2 /

PERMX

4500*15.0 /

PERMY

4500*15.0 /

PERMZ

4500*15.0 /

--Depth of cell centers

MIDS

4500*9840 /

```
PROPS
============================================================

Include

new.pvo /

-- Boiling point temperatures Deg R

TBOIL

   350.46000    139.32000    201.06000    332.10000    415.98000

   523.33222    689.67140    958.31604   1270.40061            /

-- Reference temperatures Deg R

TREF

   527.40000    140.58000    201.06000    329.40000    415.80000

   526.05233    519.67000    519.67000    519.67000            /

-- Reference densities LB/FT3

DREF

    48.50653     50.19209     26.53189     34.21053     36.33308

    37.87047     45.60035     50.88507     55.89861            /

--Water saturation functions

SWFN

--SWAT   KRW    PCOW

 0.20   0.000   0

 0.24   0.003   0

 0.28   0.010   0

 0.32   0.023   0

 0.36   0.040   0

 0.40   0.063   0

 0.44   0.090   0

 0.48   0.123   0
```

```
  0.52   0.160   0
  0.56   0.203   0
  0.60   0.250   0
  0.64   0.303   0
  0.68   0.360   0
  0.72   0.423   0
  0.76   0.490   0
  0.80   0.563   0
  0.84   0.640   0
  0.88   0.723   0
  0.92   0.810   0
  0.96   0.903   0
  1.00   1.000   0
/
SGFN
--Gas saturation functions (you may change these)
--SGAS   KRG    PCOG
   0.00  0.000  0
   0.05  0.000  0
   0.10  0.004  0
   0.15  0.015  0
   0.20  0.033  0
   0.25  0.059  0
   0.30  0.093  0
   0.35  0.133  0
   0.40  0.181  0
   0.45  0.237  0
```

0.50 0.300 0

0.55 0.370 0

0.60 0.448 0

0.65 0.533 0

0.70 0.626 0

0.75 0.726 0

0.8 0.834 0

/

SOF3

--Oil saturation functions(you may change these)

--SOIL KROW KROG

0.00 0.000 0.000

0.30 0.000 0.000

0.33 0.005 0.005

0.36 0.018 0.018

0.39 0.038 0.038

0.42 0.064 0.064

0.45 0.096 0.096

0.48 0.133 0.133

0.51 0.175 0.175

0.54 0.223 0.223

0.57 0.275 0.275

0.60 0.333 0.333

0.63 0.395 0.395

0.66 0.462 0.462

0.69 0.533 0.533

0.72 0.609 0.609

```
  0.75   0.690   0.690
  0.78   0.775   0.775
  0.80   0.834   0.834
/
--Rock and water pressure data
ROCK
5169 0.000004 /
PVTW
5169 1.0 0.000003 0.31 0.0 /
--Surface density of water
DENSITY
1* 63.0 1* /
SOLUTION
============================================================
--Request initial state solution output
OUTSOL
--Solution output for GRAF (you may change these and add more performance indicators)
PRESSURE SOIL SWAT SGAS XMF YMF ZMF /
RPTSOL
PRESSURE SOIL SWAT SGAS PSAT /
FIELDSEP
1 60.0 14.7 /
/
EQUIL
9840 5169 9940 /
```

SUMMARY
==========

--Request field GOR, water cut oil rate and total, gas rate

ALL

FGOR

FWCT

FOPR

FOPT

FWPR

FOSAT

FOE

FXMF

2 /

FYMF

2 /

FCMPT

2 /

FCMIT

2 /

BOVIS

30 30 5 /

1 1 1 /

20 20 5 /

10 10 5

1 1 5 /

10 10 1 /

20 20 1 /

30 30 1 /

/

BODEN

30 30 5 /

1 1 1 /

20 20 5 /

10 10 5

1 1 5 /

10 10 1 /

20 20 1 /

30 30 1 /

/

BGVIS

30 30 5 /

1 1 1 /

20 20 5 /

10 10 5

1 1 5 /

10 10 1 /

20 20 1 /

30 30 1 /

/

BGDEN

30 30 5 /

1 1 1 /

20 20 5 /

10 10 5

1 1 5 /

10 10 1 /

20 20 1 /

30 30 1 /

/

BPR

30 30 5 /

1 1 1 /

20 20 5 /

10 10 5

1 1 5 /

10 10 1 /

20 20 1 /

30 30 1 /

/

BOSAT

30 30 5 /

1 1 1 /

20 20 5 /

10 10 5 /

1 1 5 /

10 10 1 /

20 20 1 /

30 30 1 /

/

BGSAT

30 30 5 /

1 1 1 /

20 20 5 /

10 10 5

1 1 5 /

10 10 1 /

20 20 1 /

30 30 1 /

/

BXMF

30 30 5 2 /

/

BYMF

30 30 5 2 /

/

RUNSUM

RPTONLY

SCHEDULE
==========

--AIMCON

--6* -1 /

--Request FIP reports, group, sep and well data, and solution maps.

SAVEEND

RPTPRINT

0 1 0 1 1 1 0 1 0 0 /

```
--Specify solution maps of pressure and saturations
RPTSCHED
PRESSURE SOIL SWAT SGAS XMF YMF BXMF BYMF /
--One stage separator conditions
SEPCOND
Sep Field 1 60 14.7 /
/
--Define injection and production wells
--2000a WELLSPEC is used for back-compatibility, prefered keyword is WELSPECS
--WELLSPEC
WELSPECS
INJECTOR G1   1 1  1* GAS  /
PRODUCER G2 30 30  1* OIL  /
/
--2000a uses WELSEPC to associate separator with wells
WSEPCOND
PRODUCER SEP /
/
--2000a WELLCOMP is for back-compatibility, prefered keyword is COMPDAT
COMPDAT
INJECTOR   1  1   1  1    OPEN  1*  0.3/
PRODUCER  30  30  5  5    OPEN  1*  0.3 /
/
--Well CONTROL PRODUCER on MIN oil rate of 60 stb/day, with min bhp of 2000 psi
--2000a WELLPROD is for back-compatibility, prefered keyword is WCONPROD
WCONPROD
PRODUCER  OPEN BHP 1* 1* 1000 1* 1* 2000  /
```

/

WELLSTRE

SOURGAS 0.0744 0.0735 0.0081 0.8303 0.0130 0.0007 /

/

--2000a WELLINJE is for back-compatibility, prefered keyword is WCONINJE

WCONINJE

INJECTOR GAS OPEN BHP 2000 1* 5200 /

/

WINJGAS

INJECTOR STREAM SOURGAS /

/

TSTEP

200*4

/

END

NEW.PVO

ECHO

-- Units: F

RTEMP

--

-- Constant Reservoir Temperature

--

212

/

EOS

```
--
-- Equation of State (Reservoir EoS)
--
  PR3
/

NCOMPS
--
-- Number of Components
--
     9
/
PRCORR
--
-- Modified Peng-Robinson EoS
--
CNAMES
--
-- Component Names
--
  'CO2'
  'H2S'
  'H2O'
  'C1'
  'C2'
  'C3'
  'C5'
```

'C6+'

'C9+'

/

MW

--

-- Molecular Weights (Reservoir EoS)

--

44.01

34.076

18.01

16.043

30.07

44.097

72.151

93

250

/

OMEGAA

--

-- EoS Omega-a Coefficient (Reservoir EoS)

--

0.457235529

0.457235529

0.457235529

0.457235529

0.457235529

0.457235529

0.457235529

0.457235529

0.457235529

/

OMEGAB

--

-- EoS Omega-b Coefficient (Reservoir EoS)

--

0.077796074

0.077796074

0.077796074

0.077796074

0.077796074

0.077796074

0.077796074

0.077796074

0.077796074

/

-- Units: R

TCRIT

--

-- Critical Temperatures (Reservoir EoS)

--

548.46

672.48

473.243220390429

343.08

549.774

665.64

838.62

957.031379795428

1389.14187729794

/

-- Units: psia

PCRIT

--

-- Critical Pressures (Reservoir EoS)

--

1071.33110996644

1296.17837995939

1447.6419830194

667.78169597908

708.342379977809

615.75820998071

487.169084984738

469.530587439538

207.897699472653

/

-- Units: ft3 /lb-mole

VCRIT

--

-- Critical Volumes (Reservoir EoS)

--

1.50573518513559

1.56980902280093

0.966105060919576

1.56980902280093

2.37073199361773

3.20369188326721

4.96572241906417

5.96026538012763

15.7936339717738

/

ZCRIT

--

-- Critical Z-Factors (Reservoir EoS)

--

0.274077797373227

0.281954299174958

0.275389657034295

0.284729476628582

0.284634795100356

0.276164620041118

0.268808776316087

0.272489522668694

0.220257977984354

/

SSHIFT

--

-- EoS Volume Shift (Reservoir EoS)

--

-0.04273033674

-0.102597838

-0.07750138148

0.01426352445

-0.1442656189

-0.103268354

-0.07750138148

-0.07750138148

-0.07750138148

/

ACF

--

-- Acentric Factors (Reservoir EoS)

--

0.225

0.1

0.638993310750738

0.013

0.0986

0.1524

0.2413

0.295361989252004

0.812402803713028

/

BIC

--

-- Binary Interaction Coefficients (Reservoir EoS)

--

0.096

0 0

0.1 0.05 0

0.1 0.05 0 0

0.1 0.05 0 0 0

0.1 0.05 0 0 0 0

0.1 0.05 0 0.03264833333 0.01 0.01 0

0.1 0.05 0 0.05123 0.01 0.01 0 0

/

PARACHOR

--

-- Component Parachors

--

78

80

80.428

77

108

150.3

228.9

290.4

643.3335

/

-- Units: ft3 /lb-mole

VCRITVIS

--

-- Critical Volumes for Viscosity Calc (Reservoir EoS)

--

1.50573518513559

1.56980902280093

0.966105060919576

1.56980902280093

2.37073199361773

3.20369188326721

4.96572241906417

5.96026538012763

15.7936339717738

/

ZCRITVIS

--

-- Critical Z-Factors for Viscosity Calculation (Reservoir EoS)

```
--
   0.274077797373227
   0.281954299174958
   0.275389657034295
   0.284729476628582
   0.284634795100356
   0.276164620041118
   0.268808776316087
   0.272489522668694
   0.220257977984354
/

LBCCOEF
--
-- Lorentz-Bray-Clark Viscosity Correlation Coefficients
--
    0.1023 0.023364 0.058533 -0.040758 0.0093324
/
--PVTi--Please do not alter these lines
--PVTi--as PVTi can use them to re-create the fluid model
--PVTiMODSPEC
============================================================
--PVTiTITLE
--PVTiModified System: From Automatically created during keyword export
--PVTiVERSION
--PVTi  2010.1          /
--PVTiFPE
--PVTiNCOMPS
```

--PVTi 9 /

--PVTiEOS

--PVTi PR3 /

--PVTiPRCORR

--PVTiLBC

--PVTiOPTIONS

--PVTi 0 0 0 0 0 0 1 0 0 0 0 0 0 0 0 0 0 0 0 0

--PVTi/

--PVTiNOECHO

--PVTiMODSYS

==========

--PVTiUNITS

--PVTi FIELD ABSOL PERCENT /

--PVTiDEGREES

--PVTi Fahrenheit /

--PVTiSTCOND

--PVTi 60.0000 14.6959 /

--PVTiLNAMES

--PVTi CO2

--PVTi H2S

--PVTi 1*

--PVTi C1

--PVTi C2

--PVTi C3

--PVTi C5

--PVTi 1*

--PVTi 1*

--PVTi /

--PVTiCNAMES

--PVTi 1*

--PVTi 1*

--PVTi H2O

--PVTi 1*

--PVTi 1*

--PVTi 1*

--PVTi 1*

--PVTi C6+

--PVTi C9+

--PVTi /

--PVTiTCRIT

--PVTi 8.878998547E+01 2.128099822E+02 1.357320785E+01 -1.165900091E+02

--PVTi 9.010398544E+01 2.059699824E+02 3.789499778E+02 4.973613544E+02

--PVTi 9.294718405E+02 /

--PVTiPCRIT

--PVTi 1.071331110E+03 1.296178380E+03 1.447641983E+03 6.677816960E+02

--PVTi 7.083423800E+02 6.157582100E+02 4.871690850E+02 4.695305875E+02

--PVTi 2.078976995E+02 /

--PVTiVCRIT

--PVTi 1.505735240E+00 1.569809080E+00 9.661050961E-01 1.569809080E+00

--PVTi 2.370732080E+00 3.203692000E+00 4.965722600E+00 5.960265597E+00

--PVTi 1.579363455E+01 /

--PVTiZCRIT

--PVTi 2.740777974E-01 2.819542992E-01 2.753896570E-01 2.847294766E-01

--PVTi 2.846347951E-01 2.761646200E-01 2.688087763E-01 2.724895227E-01

--PVTi 2.202579780E-01   /

--PVTiVCRITVIS

--PVTi 1.505735240E+00 1.569809080E+00 9.661050961E-01 1.569809080E+00

--PVTi 2.370732080E+00 3.203692000E+00 4.965722600E+00 5.960265597E+00

--PVTi 1.579363455E+01   /

--PVTiZCRITVIS

--PVTi 2.740777974E-01 2.819542992E-01 2.753896570E-01 2.847294766E-01

--PVTi 2.846347951E-01 2.761646200E-01 2.688087763E-01 2.724895227E-01

--PVTi 2.202579780E-01   /

--PVTiSSHIFT

--PVTi -4.273033674E-02 -1.025978380E-01 -7.750138148E-02 1.426352445E-02

--PVTi -1.442656189E-01 -1.032683540E-01 -7.750138148E-02 -7.750138148E-02

--PVTi -7.750138148E-02   /

--PVTiACF

--PVTi 2.250000000E-01 1.000000000E-01 6.389933108E-01 1.300000000E-02

--PVTi 9.860000000E-02 1.524000000E-01 2.413000000E-01 2.953619893E-01

--PVTi 8.124028037E-01   /

--PVTiMW

--PVTi 4.401000000E+01 3.407600000E+01 1.801000000E+01 1.604300000E+01

--PVTi 3.007000000E+01 4.409700000E+01 7.215100000E+01 9.300000000E+01

--PVTi 2.500000000E+02   /

--PVTiZI

--PVTi 5.000000000E+00 1.500000000E+01 6.100000000E-01 4.500000000E+01

--PVTi 5.000000000E+00 5.000000000E+00 5.000000000E+00 1.000000000E+01

--PVTi 9.390000000E+00   /

--PVTiTBOIL

--PVTi -1.092100093E+02 -7.537001018E+01 -1.470587609E+02 -2.587900053E+02

--PVTi -1.273900088E+02 -4.369001102E+01 9.094998541E+01 1.804962773E+02

--PVTi 6.264926064E+02   /

--PVTiTREF

--PVTi 6.772998603E+01 -7.519001019E+01 6.000000000E+01 -2.586100053E+02

--PVTi -1.302700087E+02 -4.387001101E+01 6.772998603E+01 6.000000000E+01

--PVTi 6.000000000E+01   /

--PVTiDREF

--PVTi 4.850653269E+01 6.199097421E+01 4.796390637E+01 2.653188725E+01

--PVTi 3.421052756E+01 3.633307854E+01 3.893008209E+01 4.488050810E+01

--PVTi 5.316633474E+01   /

--PVTiPARACHOR

--PVTi 7.800000000E+01 8.000000000E+01 8.042800000E+01 7.700000000E+01

--PVTi 1.080000000E+02 1.503000000E+02 2.289000000E+02 2.904000000E+02

--PVTi 6.433335000E+02   /

--PVTiHYDRO

--PVTi N N N H H H H H H

--PVTi /

--PVTiBIC

--PVTi   9.600000000E-02

--PVTi   0.000000000E+00 0.000000000E+00

--PVTi   1.000000000E-01 5.000000000E-02 0.000000000E+00

--PVTi   1.000000000E-01 5.000000000E-02 0.000000000E+00 0.000000000E+00

--PVTi   1.000000000E-01 5.000000000E-02 0.000000000E+00 0.000000000E+00

--PVTi   0.000000000E+00

--PVTi   1.000000000E-01 5.000000000E-02 0.000000000E+00 0.000000000E+00

--PVTi   0.000000000E+00 0.000000000E+00

--PVTi   1.000000000E-01 5.000000000E-02 0.000000000E+00 3.264833333E-02

--PVTi 1.000000000E-02 1.000000000E-02 0.000000000E+00

--PVTi 1.000000000E-01 5.000000000E-02 0.000000000E+00 5.123000000E-02

--PVTi 1.000000000E-02 1.000000000E-02 0.000000000E+00 0.000000000E+00

--PVTi /

--PVTiSALINITY

--PVTi ZI 0.000 /

--PVTi /

--PVTiSPECHA

--PVTi 4.729150800E+00 7.628741240E+00 -4.903644934E-01 4.597785500E+00

--PVTi 1.291918014E+00 -1.008885504E+00 -1.570558146E+00 -2.378869598E+00

--PVTi 2.500946616E+00 /

--PVTiSPECHB

--PVTi 9.744900480E-03 1.905457120E-04 1.010474646E-02 6.915907040E-03

--PVTi 2.363244520E-02 4.064355960E-02 6.594128940E-02 7.575461352E-02

--PVTi 1.883349767E-01 /

--PVTiSPECHC

--PVTi -4.129676758E-06 1.792819328E-06 -2.905965873E-06 8.824032630E-07

--PVTi -5.114547902E-06 -1.169165894E-05 -1.956841655E-05 -1.456342638E-05

--PVTi -4.166119895E-05 /

--PVTiSPECHD

--PVTi 7.023679600E-10 -4.816237440E-10 0.000000000E+00 -4.636038080E-10

--PVTi 3.568356872E-10 1.316683960E-09 2.258225616E-09 0.000000000E+00

--PVTi 0.000000000E+00 /

--PVTiHEATVAPS

--PVTi 1.802570424E+04 3.433428736E+04 2.314659362E+03 0.000000000E+00

--PVTi 1.650621600E+04 3.603408601E+04 4.193916852E+04 8.392181667E+04

--PVTi 2.062596021E+05 /

--PVTiCALVAL

--PVTi 0.000000000E+00 0.000000000E+00 2.091961153E+03 1.891038000E+03

--PVTi 3.323854000E+03 4.754344000E+03 7.615324000E+03 1.012042600E+04

--PVTi 2.611416814E+04   /

--PVTi--End of PVTi generated section--

ZI

--

-- Overall Composition

--

0.05

0.15

0.0061

0.45

0.05

0.05

0.05

0.1

0.0939

/